# EVALUATION OF INORGANIC, HYDROGEN MEMBRANES AT ELEVATED TEMPERATURES AND PRESSURES

by

Bryan D. Morreale

BS Chemical Engineering, University of Pittsburgh, 1999

Submitted to the Graduate Faculty of

University of Pittsburgh in partial fulfillment

of the requirements for the degree of

Masters of Science in Chemical Engineering

University of Pittsburgh

2002

UNIVERSITY OF PITTSBURGH

SCHOOL OF ENGINEERING

This thesis was presented

by

Bryan David Morreale

It was defended on

December 20, 2001

and approved by

Robert M. Enick, Professor and MacLeod Faculty Fellow, Department of Chemical and Petroleum Engineering

Anthony V. Cugini, Adjunct Research Associate Professor, Department of Chemical and Petroleum Engineering

Badie I. Morsi, Professor, Department of Chemical and Petroleum Engineering
[Thesis Advisor]

**EVALUATION OF INORGANIC, HYDROGEN MEMBRANES AT ELEVATED TEMPERATURES AND PRESSURES**

Bryan D. Morreale, MS

University of Pittsburgh, 2002

A membrane reactor with the capability of simultaneous high-pressure, high-temperature hydrogen permeation testing has been fabricated at the National Energy Technology Laboratory (NETL) in conjunction with the University of Pittsburgh and Parsons Project Services Incorporated. The design of the hydrogen membrane testing (HMT) unit allows for hydrogen membrane evaluation at pressures and temperatures up to 3100 kPa and 1173 K, respectively. The permeability experiments conducted with the NETL's HMT unit include membrane materials, such as palladium, tantalum, Inconel 600 and a cermet membrane fabricated by Argonne National Laboratories (ANL).

The hydrogen permeability of palladium was found to be proportional to the partial pressure drop of hydrogen across the membrane to an exponent value of 0.63, $\Delta P^{0.63}$. The exponent is indicative of the mass transport of hydrogen being influenced more so by bulk diffusion (n=0.5) rather than surface dissociation (n=1). This exponential range is in good agreement with the only prior study of palladium permeability at elevated pressures, n=0.68 (Hurlbert and Konecny, 1961). The permeability data collected for the palladium membrane can be described by an Arrhenius-type expression where $9.29 \times 10^{-7}$ mol $H_2$ $m^{-1}s^{-1}Pa^{-n}$ and 37.5 kJ $mol^{-1}$, representing the pre-exponential factor and the activation energy of permeation, respectively.

The palladium permeability was also determined by assuming the partial pressure of hydrogen across the membrane to the power of 0.5, $\Delta P^{0.5}$. The permeability results appear to be in excellent agreement with the previously published correlations which assumed an exponent of 0.5 and were developed over lower temperature and/or pressure ranges than this study. The permeability of palladium obtained using this assumption can be described by an Arrhenius-type expression where $3.40 \times 10^{-7}$ mol $H_2$ $m^{-1}s^{-1}Pa^{-0.5}$ and 17.29 kJ $mol^{-1}$, for the pre-exponential factor and the activation energy of permeation, respectively.

High temperature, high-pressure experiments have also been carried out with bulk metal materials including tantalum and Inconel Alloy 600 as well as a cermet membrane fabricated by Argonne National Laboratory. The permeability results of these membranes are described both by a constrained partial pressure exponent of 0.5 and a "best-fit" value which better describes the hydrogen transport resistances the individual membranes.

ACKNOWLEDGMENTS

I would like to take this opportunity to express my appreciation and gratitude to my advisor Dr. Badie Morsi and my co-advisor Dr. Robert Enick for their encouragement and guidance throughout the duration of this work. I am also grateful to Dr. Bret Howard, Dr. Kurt Rothenberger, and Dr. Anthony Cugini for their guidance, approachability, and assistance throughout the duration of the Hydrogen Membrane Testing (HMT) project at the National Energy Technology Laboratory.

I would also like to take this opportunity to recognize Ron Hirsh, Ray Rokicki, and Jeremy Brannen, as well as the other technicians of Parsons Project Services Incorporated. Without their mechanical and technical support in the development of the test apparatus and their long hours of testing this project would never had evolved.

I wish to express my gratitude to the University of Pittsburgh, the United States Department of Energy, and Parsons Project Services Incorporated for their resources and financial support throughout the duration of the HMT project.

Finally, I would be honored to dedicate this work to my Mother. This opportunity would not have been feasible without all of the sacrifices that she made over the years. Thank you Mom!!

## TABLE OF CONTENTS

## LIST OF TABLES

## LIST OF FIGURES

# 1.0 INTRODUCTION AND BACKGROUND

Environmental concerns and regulations, as we embark on the 21st century, have propelled industry, academia and the U.S. government to investigate alternative sources and types of fuels. Hydrogen has a great deal of potential in clean fuel technology, as a combustible fuel, or in fuel cell applications. The advantage of using hydrogen is that it burns cleaner than conventional fuels, with water being the primary product upon combustion in air.

$$2H_2 + O_2 \leftrightarrow 2H_2O \qquad (1\text{-}1)$$

There are several technologies for the manufacture of hydrogen and its separation from gas mixtures. Some of the most common, commercial hydrogen separation technologies are cryogenic separation, pressure swing adsorption, polymer membrane diffusion and catalytic purification (Netherlands et al. 1995, Grashoff et al.1983)*. In this study, however, selective diffusion technologies are being investigated by the application of a high-pressure, high-temperature inorganic membrane reactor for the production of highly pure hydrogen.

Recently, a hydrogen membrane testing (HMT) unit has been designed and constructed at the National Energy Technology Laboratory (NETL) to evaluate various hydrogen membranes as high-pressures and temperatures. The HMT unit is suitable for analyzing the permeation characteristics of hydrogen through different membrane materials at total pressure drops exceeding 3100kPa and temperatures as high as 1173K. The interest in the high-pressure, high-temperature studies is primarily related to the conditions associated with the gasifier products,

* Parenthetical references with years refer to bibliography.

which will be directed to a membrane reactor in a Vision 21 power plant as depicted by Figure 1 (Combustion Engineering, 1993).

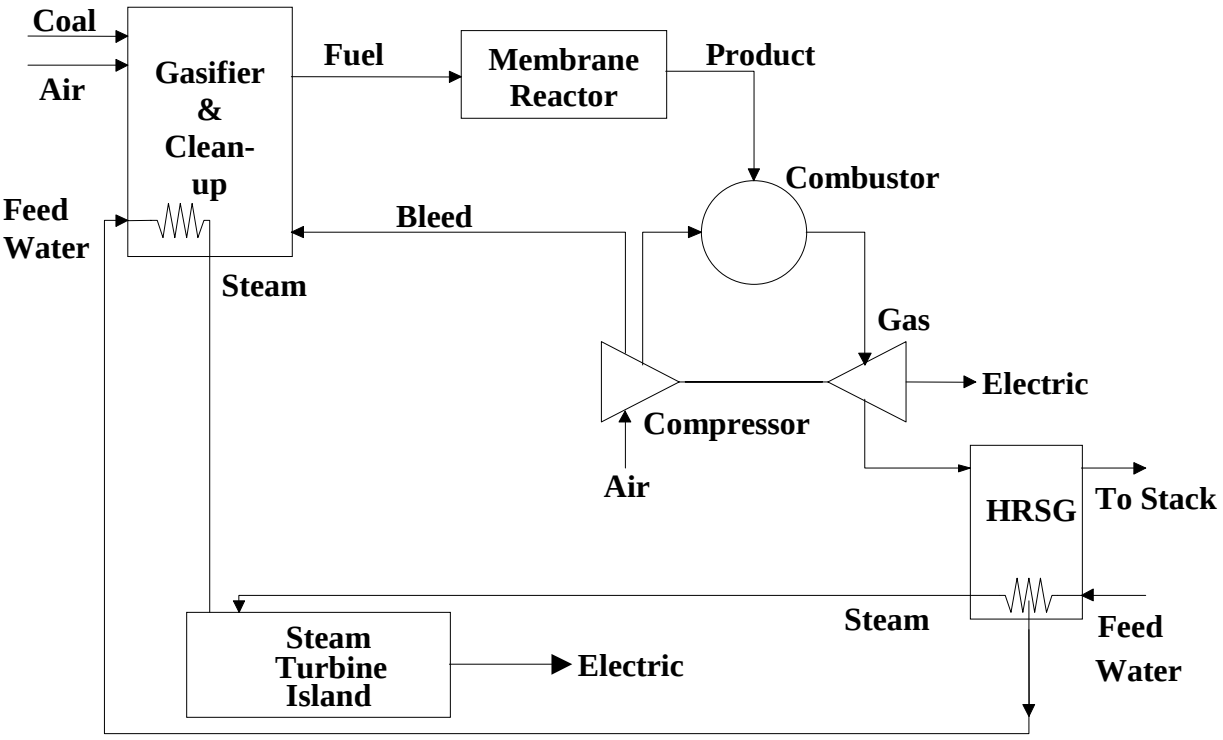


**Figure 1 Simplified schematic of the Integrated Gasification Combined Cycle.**

Gasification, is a combustion process that mainly produces a fuel gas mixture of carbon monoxide, carbon dioxide, hydrogen and trace contaminants including hydrogen sulfide, ammonia, halides and fly ash (Netherlands et al. 1995, Fain et al. 1992). The fuel stream, rich in carbon monoxide, can be further reacted with steam to promote conversion of carbon monoxide to hydrogen and carbon dioxide, which is known as the water-gas shift (WGS) reaction as given below.

$$CO + H_2O \leftrightarrow H_2 + CO_2 \qquad (1\text{-}2)$$

The WGS reaction is an exothermic reaction whose equilibrium conversion is favored at low temperatures. The promotion of the WGS reaction at elevated conditions associated with the combustion process is of interest due to the potential for high hydrogen production and carbon monoxide consumption. The common approach for application of the WGS reaction for hydrogen production (high CO conversion) has been to decrease the temperature in presence of a catalyst to favor the formation of hydrogen by enhancing the kinetics (Netherlands et al. 1995). This approach, however, increases the costs associated with the additional utilities and catalyst. Thus, the use of a high temperature, high pressure membrane reactor to the gasification-WGS system would lead to improved overall process efficiency due to circumventing the need for a catalyst and cooling of the fuel gas stream. The membrane reactor would also shift the equilibrium of the reaction towards the production of hydrogen and $CO_2$ as a result of the extraction of hydrogen through the inorganic membrane (Enick et al., 2000). Therefore, a selective, stable, highly permeable hydrogen membrane that could withstand the elevated pressures and temperatures associated with gasification product streams must be identified. The application of a mechanically stable membrane reactor would have two effluent streams, a high purity, low-pressure hydrogen stream and a high-pressure water/carbon dioxide stream. The high-purity hydrogen stream could serve as a chemical feedstock, a fuel or a feed stream for a hydrogen fuel cell. The water/carbon dioxide stream on the other hand could be cooled to condense the water thus directing the high-pressure carbon dioxide to a sequestration system.

Enick et al. (2000) proposed that the application of the WGS reaction to a high-pressure, high-temperature membrane reactor can increase the conversion of CO from 35% to almost 80% assuming a membrane thickness of 1mm, and process conditions of 1173K with a membrane pressure gradient of 2635kPa. The model showed that permeate side of the membrane

maintained at 101kPa in absence of a sweep gas would impure the permeating hydrogen. In addition, the conversion of CO approached 100% in the model if the partial pressure of hydrogen on the permeate side is reduced by using a vacuum or a sweep gas.

Many metals, such as palladium and a selection of the refractory metals, such as niobium, tantalum, vanadium and zirconium, have shown high diffusion capabilities with respect to hydrogen (Steward et al. 1983). Palladium was selected as the membrane material for the verification of the NETL membrane reactor due to its high hydrogen permeability and highly catalytic surface. Experiments with hydrogen permeable palladium membranes began in the middle of the $19^{th}$ century by several researchers, including Deville, Troost, and Graham (Grashoff et al. 1983). Palladium is still the most common material for hydrogen membrane research at high temperatures as a result of its high hydrogen permeability, infinite hydrogen selectivity, reasonable mechanical characteristics, and highly catalytic surface which dissociates hydrogen molecules rapidly. Table 1 illustrates literature values for the bulk palladium/hydrogen system and as can be noted, a majority of the studies were conducted above 573K to avoid the phase transition, which causes mechanical failure of the membranes. Palladium undergoes an $\alpha$-$\beta$ phase transition at temperatures below 573K and pressures below 2027kPa. The $\alpha$-palladium hydride phase is the occurring crystalline phase of the metal at low hydrogen concentrations, however, the presence of increased hydrogen concentrations below 573K and 2027kPa leads to the formation of the $\beta$-palladium hydride phase. The co-existence of the $\alpha$-$\beta$-palladium phases can result in significant material strains due to the expanded crystalline lattice of the $\beta$-palladium hydride phase as compared to the $\alpha$-phase. Moreover, cycling the palladium membrane through the $\alpha$-$\beta$ phase transition region can result in distortion and severe embrittlement, thus reducing the palladium membrane life significantly (Grashoff et al. 1983).

Unfortunately, palladium is also extremely expensive ($1000 per troy ounce), roughly four times the cost of gold, making it an impractical bulk material for reactor construction (NYMEX, 1/2001). Therefore, an economically feasible, palladium based, commercial scale system would require a significantly reduced amount of palladium. The high cost of palladium has propelled membrane research to develop techniques to use the characteristics that make palladium such an advantageous membrane without the costs associated with it. Thus, a methodology of obtaining the advantageous membrane characteristics of palladium without the associated costs is by utilizing a reduced amount of palladium. The reduction of palladium content used in membrane construction has been sought after by many methods including alloying, coating and composite membranes.

**Table 1 Summary of literature permeation values of palladium.**

| **Researcher** | **Composition** | **$t_M$** (μm) | **T** (K) | **$P_{TOT,Ret}$** (kPa) | **$P_{TOT,Per}$** (kPa) | **$P_{H2,Ret}$** (kPa) | **$P_{H2,Per}$** (kPa) | **$k_O$** (mol $m^{-1}s^{-1}Pa^{-0.5}$) | **$E_P$** KJ $mol^{-1}$ |
|---|---|---|---|---|---|---|---|---|---|
| Balavnev et al. 1974 | Bulk Pd | 100-1000 | 370-900 | $3x10^{-8}$-$7x10^{-5}$ | 101.3 | $3x10^{-8}$-$7x10^{-5}$ | 101.3 | $1.89x10^{-7}$ | 15.46 |
| Davis et al. 1954 | Bulk Pd | 130-729 | 473-973 | $3x10^{-3}$-101 | Vacuum | $3x10^{-3}$-101 | Vacuum | $3.85x10^{-7}$ | 18.56 |
| Holleck et al. 1967 | Bulk Pd | 800-2025 | 500-900 | ~53 | 0.024-0.006 | ~53 | 0.024-0.006 | $1.64x10^{-8}$ | 12.82 |
| Hurlber et al. 1961t | Bulk Pd | 10-150 | 623-773 | 101-710 | Vacuum | 101-710 | Vacuum | $1.47x10^{-8}$ | 11.92 |
| Katsuta et al. 1979 | Bulk Pd | 940 | 769-1219 | 101 | Vacuum | 101 | Vacuum | $3.82x10^{-7}$ | 20.50 |
| Koffler et al. 1969 | Bulk Pd | 486-762 | 300-709 | $4x10^{-5}$-$7x10^{-3}$ | $1.3x10^{-8}$ | $4x10^{-5}$-$7x10^{-3}$ | $1.3x10^{-10}$ | $2.20x10^{-7}$ | 15.67 |
| Toda et al. 1958 | Bulk Pd | 11500 | 443-563 | ~84 | Vacuum | ~84 | Vacuum | $1.72x10^{-7}$ | 13.46 |

## 1.1 Palladium Alloys

Palladium alloy research has been conducted in efforts to minimize the amount of palladium needed in membrane development as well as increasing the hydrogen permeation rate. Moreover, research has identified that binary alloys of palladium can reduce the amount of distortion resulting from the α-β-palladium phase transition (Grashoff et al. 1983, Shu et al. 1991). Palladium has been the parent material for binary membranes, alloyed with an array of materials including silver, gold, copper, nickel, iron, etc. Although all the metals alloyed with palladium have some effect on permeation and deformation resistance, silver is unique in that the palladium-silver alloys can exhibit higher permeabilities than each of the bulk metals exhibit indivisually, as well as improved mechanical strengths and decreased costs. For instance, a 23%Ag/Pd alloy exhibits a permeability approximately 70% greater than pure palladium at a cost reduction of about 23% (due to the costs of silver is approximately $5 per troy ounce or 0.5% that of palladium). In this alloy, however, hydrogen permeabilities decrease as the silver content further increases. The palladium/silver alloy membrane system was successfully commercialized in the early 1960's, with an alloy composition of about 25%Ag/Pd (Grashoff et al. 1983). Although the Pd/Ag alloys have a positive economic impact on palladium-based membranes, a bulk membrane composed of 70-77% palladium would still not be a significantly cost-effective alternative for large-scale processes (Moss et al. 1998).

## 1.2 Palladium Coated Substrates

Palladium coated membranes offer a mean for reducing the amount of palladium needed. The palladium would provide a thin, stable, catalytic, highly selective hydrogen permeable coating which can be economically viable for a thickness in the micron range. The substrate

chosen for coating must exhibit the mechanical strength and integrity for the desired applications as well as high hydrogen diffusion capabilities (Li et al. 1998).

The permeation of hydrogen through palladium is inversely proportional to the thickness of the membrane, therefore the ability to develop techniques of minimizing the coating thickness is crucial in decreasing costs and increasing hydrogen permeation (Moss et al. 1998, Li et al. 1998). However, a higher rate of permeation for the composite membrane can only be realized if the membrane substrate has higher hydrogen diffusion capabilities than the coating.

A successful candidate for a composite membrane substrate must have a high diffusion rate for hydrogen atoms/ions for dense substrates or a high permeance for hydrogen molecules for porous substrates. The high substrate permeation rate would allow the rate-limiting step in the diffusion process be directly related to the hydrogen dissociation and diffusion through the ultra-thin layer of palladium.

The high substrate permeation rate can be achieved by the application of a porous substrate (Ueimya et al. 1991, Itoh et al. 1992, Li et al. 1998).The porous substrate would allow molecular hydrogen to permeate the substrate with the resistances associated with molecular-molecular and molecular-wall interactions, rather than atomic hydrogen diffusion resistances through crystalline structures. Porous stainless steel is the most common porous metal substrate considered for composite hydrogen membranes due to its mechanical properties (Shu et al. 1994). One of the major concerns associated with large-scale, palladium-coated porous substrate composite membranes is the mechanical integrity of the coating. Any defect in the palladium coating would result in leaks with poor selectivity, which would reduce the overall selectivity of the membrane. The low selectivity can be attributed to the flow of impurities form the retentate

side to the permeate side of the membrane. The selectivity of such leaks would be related to the hydrogen selectivity of the porous stainless steel substrate.

High substrate permeation rate can also be achieved by the selection of a dense substrate, which exhibits a higher permeability than palladium (Buxbaum and Kinney 1996, Moss et al. 1998). The palladium coating would provide a stable, catalytic surface for hydrogen dissociation, while the bulk material would exhibit low hydrogen diffusion resistances and increased mechanical strength (Moss et al. 1998). Several metals apparently have higher hydrogen permeabilities than palladium over a wide range of temperatures. The most notable metals are the Group V refractory metals, including niobium, tantalum, vanadium and zirconium. These refractory metals have shown the ability for higher permeation rates as estimated by previously published solubility and diffusivity data (Steward et al. 1983). However, these metals cannot be used alone in the proposed application because of the highly stable, hydrogen-impermeable oxides which form on the surface (Moss et al. 1998). The resultant is a poor catalytic surface, which does not rapidly dissociate hydrogen molecules. Therefore, palladium-coated refractory metal composite membranes have been considered because they are mechanically stronger and less expensive than palladium membranes of comparable thickness. Thus, application of these refractory metals as substrates for ultra-thin palladium deposition can reduce the amount of palladium required while increasing hydrogen permeability by reducing the surface resistance associated with the refractory metals of interest. Nonetheless, hydrogen embrittlement remains a concern for any membrane based on these metals, particularly zirconium.

### 1.3 Ceramic / Composite Ceramic Membranes

Ceramics have been considered for increasing performance while decreasing costs of hydrogen membranes. Dense membranes composed of ceramics and metals (cermets), have been

considered as ion-transport membranes. Porous ceramics have been used as substrates for palladium coating while other porous ceramic membranes have been proposed for hydrogen separation, which do not require a palladium coating. This is because the separation is based on the ability of the hydrogen molecules to migrate through the small pores of the ceramic. Porous membranes, however, cannot achieve infinite hydrogen selectivity exhibited by the dense hydrogen membranes. Moreover, sealing in each of the ceramic membrane technologies also suffers from the mechanical difficulties associated with "joining" to metal components via brazing or mechanical fittings.

### 1.3.1 Dense Cermets

Cermets are relatively a new area in hydrogen membrane technology, which involves a membrane blend of protonic/electronic mixed oxides and metals. Dense cermet membranes are known to be infinitely selective to hydrogen and are a durable alternative to palladium membranes as a result of the mechanical integrity under elevated conditions (Balachandran et al. 1998). Although palladium is an obvious selection for the metal component, other metals such as nickel have been proposed (Balachandran et al. 1998).

The cermet membranes are characterized by a transport mechanism similar to that of atomic diffusion, which occurs in palladium. Ionic-transport is the governing process in the hydrogen-cermet system. Like palladium, hydrogen gas dissociates on the surface of the membrane, not into two hydrogen atoms, but rather into hydrogen protons and electrons. The hydrogen protons and electrons then diffuse through the membrane material in the direction of decreasing concentration and then recombine on the surface of the membrane, which is at low hydrogen concentration.

### 1.3.2 Porous Ceramics

Porous ceramic membranes have been a research topic in membrane development by its application as a porous substrate for palladium coating. The methodology of coating porous ceramics mirrors that of the porous stainless steel, which was described in the previous section. The resistances associated with the porous ceramic substrate are only encountered as a result of the molecular-molecular and/or molecular-wall interactions. The resistance associated with the pore sizes of interest, 10 to 100 Angstroms, is small when compared to the resistances associated with the dissociation and migration of hydrogen through the thin layer of palladium. Thus, as a result of permeation being inversely proportional to thickness, the application of a palladium coating in the micron range would result in dissociation of hydrogen as the rate-limiting step in the process. The porous ceramic could be made thick enough to ensure the mechanical integrity needed under the proposed application.

Other porous ceramic membranes offer a method of eliminating the use of palladium as the catalytic metal in fabrication. The mechanism of hydrogen transport through porous ceramic membranes is dissimilar to any of the membranes previously discussed, in that these porous ceramics can separate hydrogen from a mixture based on the size of the molecules (hydrogen being the smallest). The porosity and pore diameters of the ceramic membranes are the governing physical characteristics of gas separation with this technology. Although these inexpensive membranes may be stable in the presence of oxidizing gases, sulfur-containing gases, and exhibit higher hydrogen fluxes than dense membranes at comparable conditions, 100% selectivity for hydrogen cannot be realized and mechanical seals must be carefully designed (Reference, Fain).

Hydrogen diffusion and selectivity in porous type ceramic membranes are influenced by the molecular diameter of the materials of interest and the pore diameter of the membranes. The flow of hydrogen through porous media is encompassed by three diffusion regimes all based on the pore diameter and the mean free path. The mean free path, $\lambda=\lambda(\mu,P,T,M)$, of a gas molecule is defined as the distance a molecule will travel before it collides with another gas molecule. Knudsen diffusion, one of the more understood diffusion processes, is the dominant transport mechanism of mass transfer when the mean free path is large when compared with the pore diameter or when the pore diameters are very small (Hill, 1977).

Since Knudsen diffusion encompasses transport mechanisms where molecular-wall interactions dominate, molecular diffusion is the mechanism where molecular-molecular interactions are most important. Molecular diffusion is thus classified as the diffusion process in which the mean free path is small when compared to the pore diameter. The last diffusion regime is described by a combination of Knudsen and molecular diffusion in which the mean free path and the pore diameter are in size ranges which encompasses the transition between the two diffusion regimes. Thus, both the molecular-molecular and the molecular-wall interactions are important (Geankopolis, 1993).

Hydrogen selectivity in ceramic type porous membranes is a direct function of the pore size and pore distribution of the membrane and the mean free path associated with the system of interest. The diameter of the pores must be large enough to promote the flow of the wanted material while small enough to reject the pollutant. Thus, equating the selectivities of porous and dense membrane technologies could only be accomplished if all of the pores had a diameter greater than the molecular diameter of the hydrogen and smaller pores than the next smallest

molecular diameter of the gas stream. Although some pore technologies can reduce the pore diameter to the required size, selectivity is still a concern because of pore size distribution.

## 2.0 RESEARCH OBJECTIVE

From this introduction it appears that permeability experiments previously conducted by Holleck et al. 1967, Katusa et al. 1979, Balavnev et al. 1974 and Davis et al. 1954 included relatively high-temperature (T>900 K), and low-pressure membrane experiments. Experiments under pressures and temperature exceeding 3100kPa and 1173K, which are the conditions associated with gasification, however are not available in the literature.

Therefore, the main objective of this study is to provide the first hydrogen permeation characteristics of inorganic membranes at high-pressures and high-temperatures (up to 3103kPa at 1173K). These conditions are similar to those of gasifier products stream. The recent interest in this technology is to remove hydrogen from fuel gas as well as attaining high conversions of the water-gas shift reaction and the steam reforming of light hydrocarbons via the removal of hydrogen from the membrane reactor.

The membrane materials used in this study include palladium, tantalum, Inconel 600 and a cermet composition for which the hydrogen permeability, $k_P$, and the partial pressure exponent, n will be evaluated. These data will allow for the production of ultra-pure hydrogen, which can be used as a chemical feedstock or a fuel.

# 3.0 EXPERIMENTAL

## 3.1 Membranes

In this study, three bulk metal membranes, Inconel 600, palladium, tantalum, and a novel cermet composition were evaluated. The majority of the membranes were fabricated as 1-mm thick, 0.625 to 0.75-inch diameter disks. The membrane materials and preparation techniques investigated in this study are as follows:

### 3.1.1 Bulk Metals

The bulk metals used in the development of the Pd and Ta membranes were obtained from Alfa AeSar. The bulk metals were purchased as 1mm thick, 50mm-x 50mm sheets, with a minimum purity of 99.9%. The membranes were then fabricated to the proper diameter, ranging from 0.625 to 0.75 inches, using a metal-punch. All of the surfaces of the bulk metal membranes were then smoothed using a series of different sandpaper, from a coarse-grit initially to a smooth-grit for the final polishing. The polishing of the bulk metal membranes allowed for better approximation of the membrane surface area as well as promoting the mounting of the membranes into the designed membrane holders, which was the next step in the membrane preparation process.

The mounting of the fabricated bulk metal membranes into the membrane reactor design was achieved using two different methods. The first method was a brazing technique developed at the NETL using a membrane holder as depicted in Figure 2. The brazing material was composed of high-purity gold powder with a boric acid flux to promote braze flow and adhesion. The mounted bulk metal membranes were heated to approximately 1473 K under an argon

atmosphere. The inert atmosphere was used to prevent the formation of additional oxides on the surface of the membrane, which can diminish hydrogen permeation.

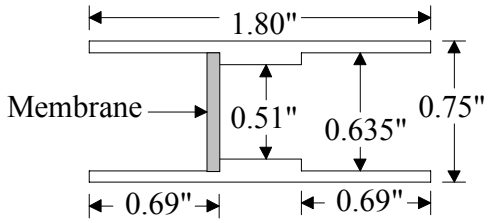


**Figure 2 Schematic of the bulk metal membrane holder for brazing methodology.**

As a result of the difference in thermal expansion coefficients of the membrane and membrane holder, the changes in temperature associated with the welding of the extension tubes and the ramping of testing conditions often resulted in membrane sealing failures. Since the overall length of the membrane holder did not changed due to the easy accessibility of the membrane while working, a second method of membrane mounting evolved. This second method involved butt-welding a 0.75-inch membrane in-between two 0.75-inch Inconel 600 tubes as illustrated in Figure 3.

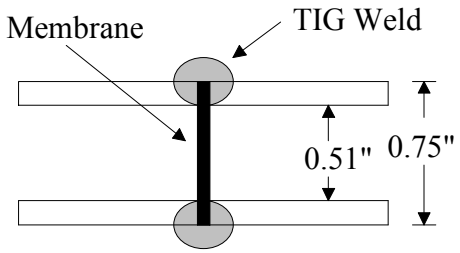


**Figure 3 Schematic of membrane holder for TIG welding methodology.**

After heating, cleaning of the mounted bulk metal membranes was conducted to eliminate any residual material from the surface. The mounted membranes were then

mechanically cleaned with a combination of stainless steel wire brushes and select grades of silicon carbide powder to remove any unwanted materials from the surface. The membranes were then chemically treated with an appropriate acid (most commonly 20vol% HNO3, 20vol% HF, 60vol%) to remove any of the surface oxides or contaminants which may have been present after the previous cleaning measures. After mounting and cleaning, the bulk metal membranes were placed in a desiccator to eliminate any further formation of oxides onto the membrane surface as well as to reduce the likelihood of contamination until testing.

### 3.1.2 Cermets

The cermet membranes provided for this study were fabricated by a process developed at Argonne National Laboratory. The ANL cermet membrane were composed of a mixture of various protonic/electronic conductivity oxides and metals. The specific composition of the ANL-1 cermet membrane was 60vol% $BaCe_{0.8}Y_{0.2}O_3$ and 40vol% metallic nickel. The ceramic bases of the ANL membranes were prepared by calcining appropriate mixtures of specific oxides at 1273K for 12 hours. The ceramic base was then ball milled and recalcined at 1473K for 10 hours. The calcination process was conducted under an air atmosphere in the both steps previously described, forming a mixed-oxide powder product. The mixed-oxide powder was then analyzed by X-ray defraction to confirm the phase purity. A specified volume of metallic and mixed oxide powder was then blended to increase the electronic conductivity of the membrane. The metal was added to the membrane composition to promote the flow of charge across the membrane. The final step in the fabrication of the cermet membranes was uniaxially pressing the cermet powder into a disk and sintering for 5 hours at 1400 to 1450$^{o}$C under a 4% hydrogen / argon atmosphere.

The membrane holder (Figure 4) for the cermet membranes were provided to ANL by the NETL. The cermet membrane was then brazed into the mount using a technique developed by

ANL. After receiving the brazed cermet membranes from ANL, the membrane surfaces were photographed and placed into a desiccator until tested.

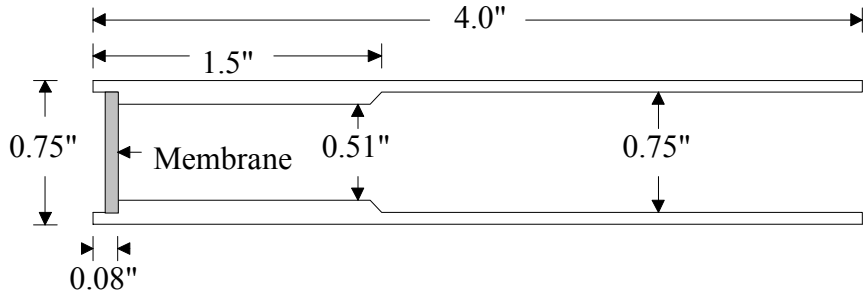


**Figure 4 Schematic of the cermet membrane holder.**

### 3.1.3 Inconel 600

The majority of the hydrogen membrane-testing unit is constructed from 316 stainless steel. However, the material of construction used for direct contact with the severe test conditions, the "hot zone", is Inconel 600. The Inconel membrane was fabricated from a 0.75-inch diameter by 5.5-inch long Inconel 600 rod. The 5.5-inch Inconel rod was drilled out from both ends to develop a 1mm thick membrane. The Inconel 600 membrane and membrane holder was therefore fabricated as one piece, as is illustrated in the schematic of Figure 5.

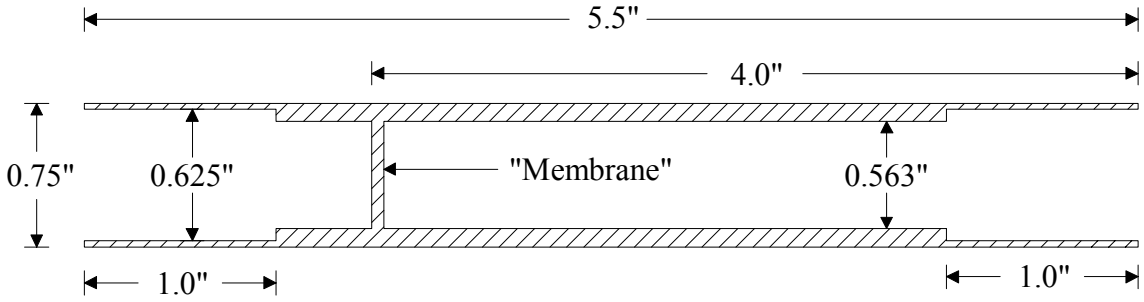


**Figure 5 Schematic of the Inconel 600 membrane and holder.**

## 3.2 Hydrogen Membrane Testing Unit

The hydrogen membrane testing (HMT) unit was constructed at the National Energy Technology Laboratory (NETL). The apparatus was designed to allow testing of inorganic hydrogen membranes at high pressures and temperatures up to 3103kPa and 1173K, respectively. A simplified schematic of the HMT unit is illustrated in Figure 6 and 7. For simplification, the HMT unit description will be divided into two sections, the reactor and the gas analysis.

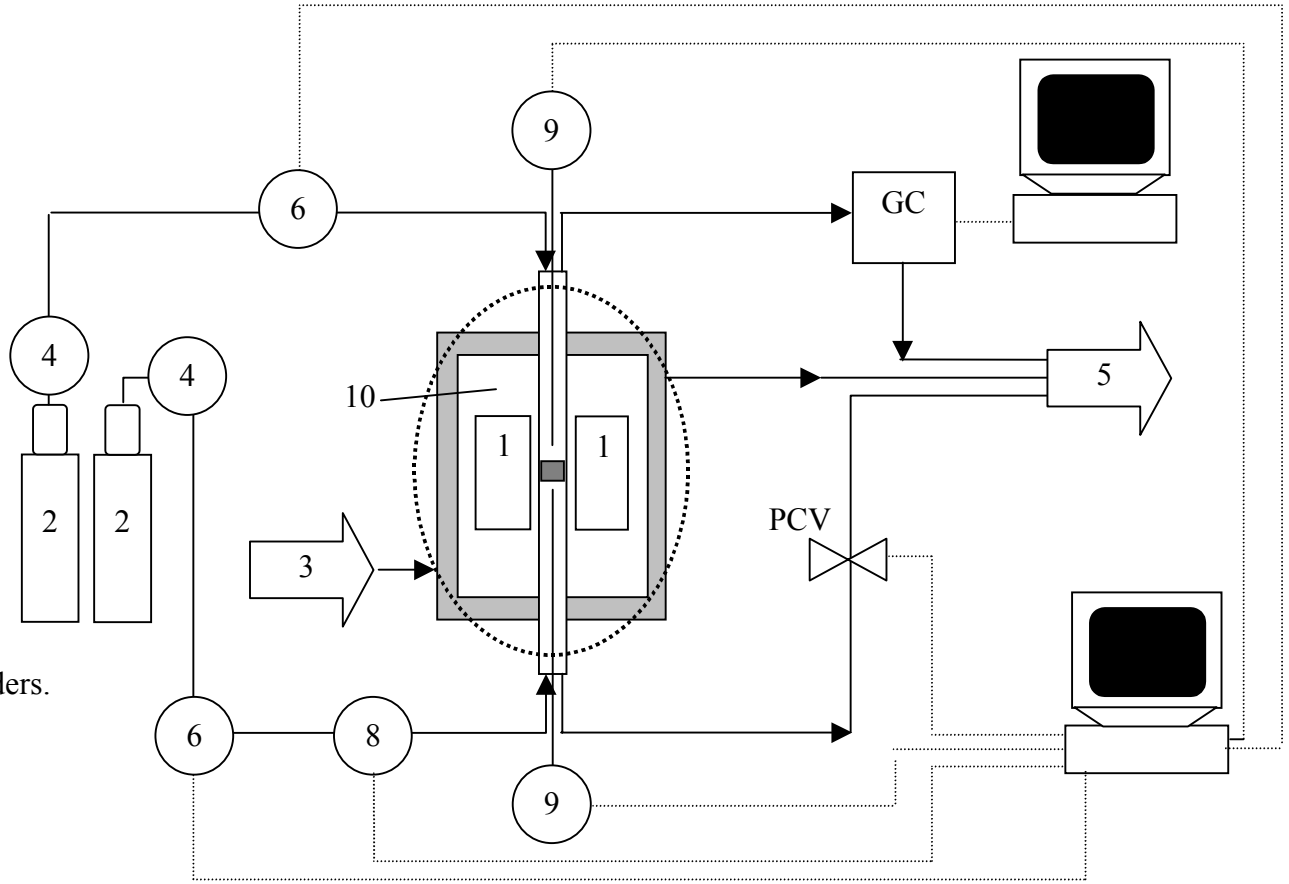


1. Resistance heater.
2. Process feed gas cylinders.
3. House-nitrogen purge.
4. Cylinder regulators.
5. Vent.
6. Flow transducer.
7. Pressure transducer.
8. Pressure control valve.
9. Thermocouple.
10. Reactor Autoclave

····· See reactor detail in Figure 6.

**Figure 6 Schematic of the experimental setup.**

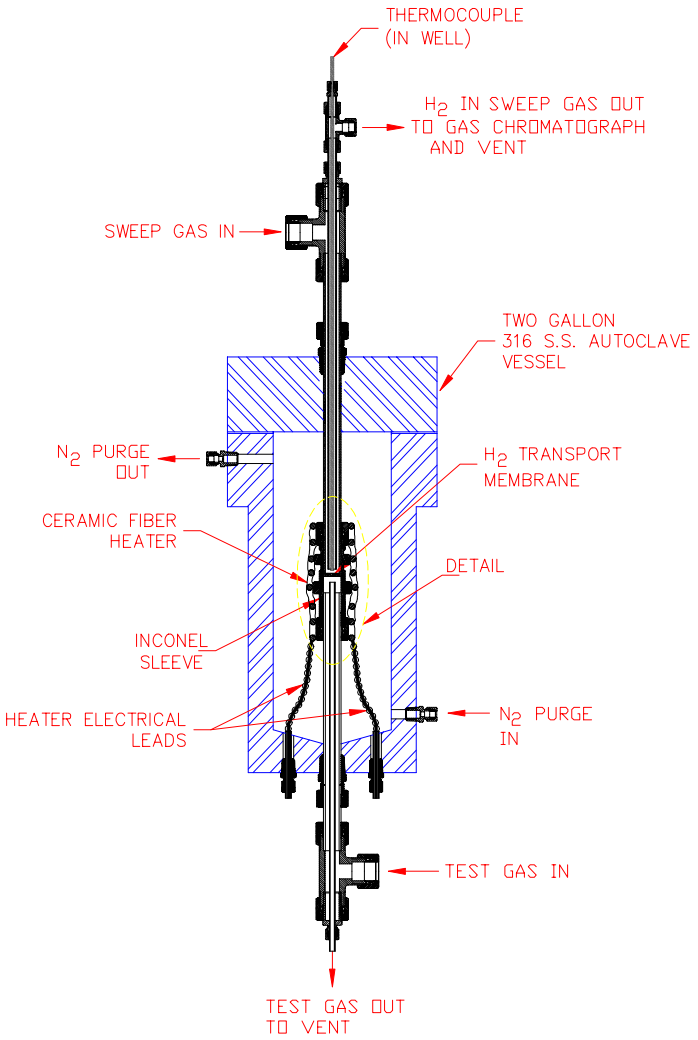


(a)

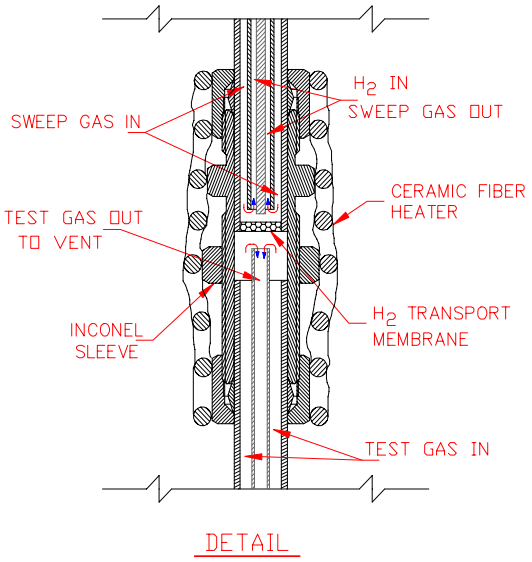


(b)

**Figure 7 Detail of the HMT reactor and Autoclave.**

### 3.2.1 HMT Reactor

The HMT reactor consisted of two 0.75-inch Inconel 600 tubes placed above and below the membrane holder as shown in Figure 8. Two methods were used to assemble the test apparatus, one for the metal membranes (Figures 3 and 4) and one for the cermet membranes (Figure 5).

The metal membranes were mounted into the membrane holders, illustrated in Figures 3 and 4. The mounted membrane and membrane holder were then welded on both ends to predetermined lengths of 0.75-inch Inconel 600 tubing. An example of this configuration is illustrated in Figure 8, assuming the brazed bulk metal membrane methodology.

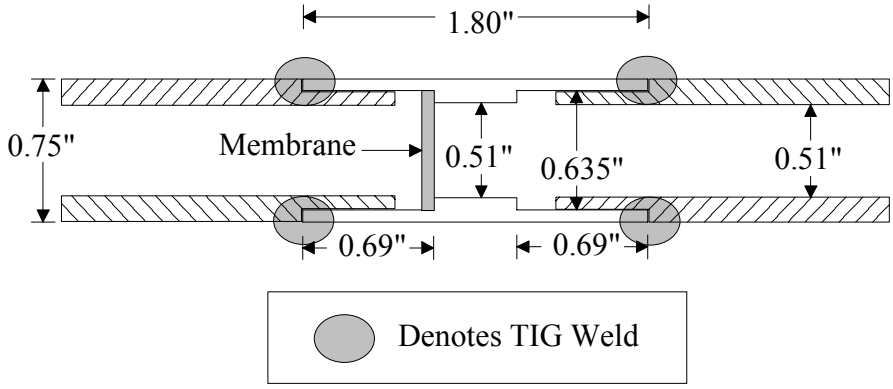


**Figure 8 Schematic of the brazed bulk metal membrane and extension tube design.**

Argonne National Laboratory brazed the cermet membrane and membrane holder, Figure 4, which was provided by the NETL. The brazed cermet membrane and membrane holder was then welded at one end to a predetermined length of 0.75-inch Inconel 600 tubing. The weld was placed at the end of the membrane holder furthest away from the membrane. The second piece of 0.75-inch Inconel 600 tubing was placed approximately 0.25 inches away from the membrane and secured to the holder with the use of a Inconel 600 Swagelock Bulkhead Union. The

bulkhead fitting was used in place of a second weld to insure the integrity of the membrane at the temperatures associated with welding. A schematic of the cermet membrane and bulkhead configuration is illustrated in Figure 9.

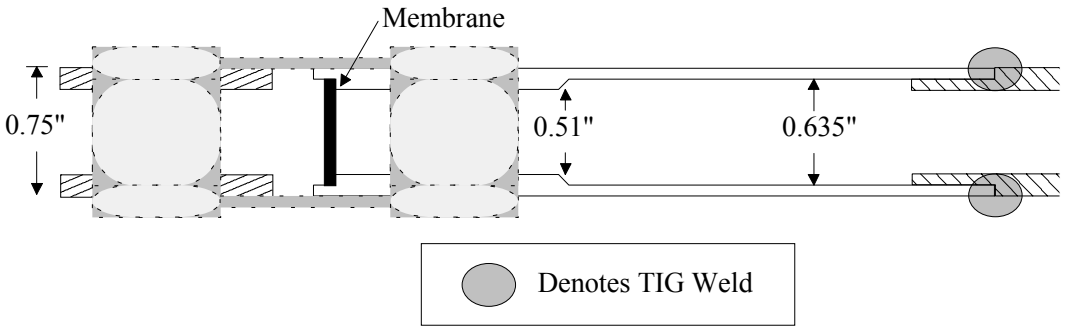


**Figure 9 Cermet membrane, Swagelock union and extension tube schematic.**

The assemblies described above consist of a predetermined length of 0.75-inch Inconel 600 tubing, an inorganic hydrogen membrane mounted in the required holder and a second piece of 0.75-inch Inconel 600 tubing in series. The reactor assembly consisted of two 0.375-inch Inconel 600 tubes, placed concentrically inside the 0.75-inch Inconel 600 tubing, approximately 0.25 inches form the membrane surface. The "tube inside a tube" configuration described allowed the feed and sweep gas to enter the reactor assembly, contact the membrane surface and exit the assembly on both the retentate and permeate side. An illustration of the "tube inside a tube" configuration is depicted in Figure 9 for all membrane testing.

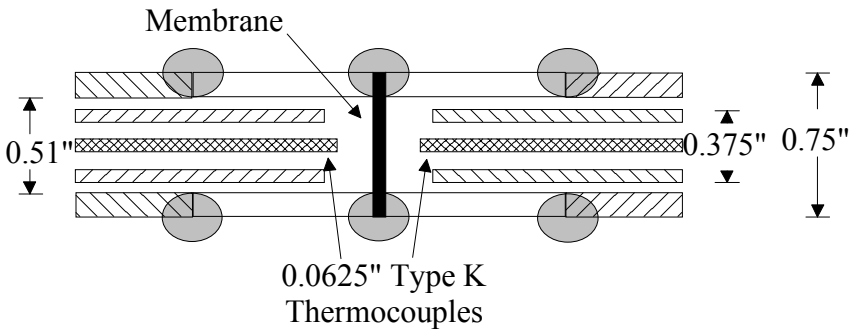


**Figure 10 Schematic of the "tube inside a tube" configuration.**

The temperature of the membrane reactor, as illustrated in Figures 6, 7, and 10 was maintained with a Watlow 120-V, 6-inch resistance heater. The heater was controlled with the use of Iconics' Genesis process control program and inline thermocouples. The thermocouples used were type-K and were placed approximately 0.25 inches from one or both sides of the membrane surface.

The membrane reactor and resistance heater were insulated with ceramic fiber insulation and placed inside a 2-gallon stainless steel autoclave pressure vessel. The 2-gallon autoclave was used for three reasons. Firstly, since hydrogen was being tested above its auto-ignition temperature (673 K), the autoclave allowed for purging of the HMT unit's hot zone. Secondly, the stainless steel autoclave was used as an environmental isolation vessel, to ensure that any amount of hydrogen that happened to escape from the reactor (via leak or permeation) would be so dilute that auto-ignition would not be a concern. Thirdly, in the event of a catastrophic situation in which a hydrogen explosion could manifest in the reactor, the 2-gallon stainless steel autoclave would prevent the propagation of shrapnel throughout the test area.

### 3.2.2 Test Gases and Analysis

The membrane reactor feed gas consisted of a known mixture of hydrogen and helium on the retentate side, while pure argon was chosen for the sweep gas of the permeate. Helium was

chosen as a balance mixture for the feed gas as a tool for identifying leaks in the membrane or the membrane system. Although the hydrogen and helium molecules are small, only the hydrogen molecule has the ability to permeate through a dense membrane via ionic- or atomic-diffusion. Thus, the detection of helium in the permeate stream would indicate a leak in the membrane or the test apparatus.

The process and sweep gases were introduced to the membrane reactor at sufficient flow rates to ensure optimal hydrogen concentrations. The hydrogen flow rate on the retentate side of the membrane was maintained at a value to ensure that the hydrogen concentration was not depleted due to permeation through the membrane. While a sweep gas was used to ensure the permeate hydrogen concentration close to zero to facilitate analysis, but high enough to be accurately and precisely detected. The process and sweep gas feed streams were fed from a cylinder, with the flow rates controlled by inline 5850i Series Brooks flow meters. The flow meters were calibrated by Brooks for the specific gases used in each stream and recorded flow rates in standard conditions. The process feed pressure was regulated by stainless steel, pneumatic Badger 807 Series Research control-valve.

The hydrogen permeating through the membrane was carried to a Hewlett Packard 5890 Series II gas chromatograph (GC) by the argon sweep stream. The argon sweep stream flow rate was regulated to maintain the hydrogen concentration within the calibration range of the GC. An excessively large flow rate would result in hydrogen concentration below the GC detection limit of approximately 20-ppm. While an insufficient sweep flow rate would result in saturation of the GC detector.

The GC was equipped with a 10-foot, zeolite packed column and was used in conjunction with a thermal conductivity detector (TCD) to obtain proper separation and analysis of the test

gases. The TCD detects based on thermal conductivity differences between the gas molecules of the test gases and the reference gas. Argon was chosen as the reference gas for the TCD to reduce the number of peaks recorded for a single injection as well as being known as the gas of choice for hydrogen detection.

The GC calibration was conducted using three gas mixtures obtained from Butler Gas Company. The compositions were 0.09, 1.94 and 5.09% hydrogen by volume, with argon representing the balance of the mixtures in each case. A GC calibration curve was constructed using five injection samples of each of the three calibration gas mixtures in conjunction with the plots origin, (zero concentration results in zero peak area). An example of a calibration curve generated for the HMT unit's GC analysis is illustrated in Figure 11, with the GC conditions chosen for calibration and testing listed in Table 2.

**Table 2 GC operating and calibration conditions.**

| | |
|---|---|
| Oven Temperature | 348K |
| Injector Temperature | 378K |
| Detector Temperature | 473K |
| Carrier and Reference Gas Composition | Argon |
| Carrier Gas Flow Rate | 32.5 ml / min |
| Reference Gas Flow Rate | 44.5 ml / min |

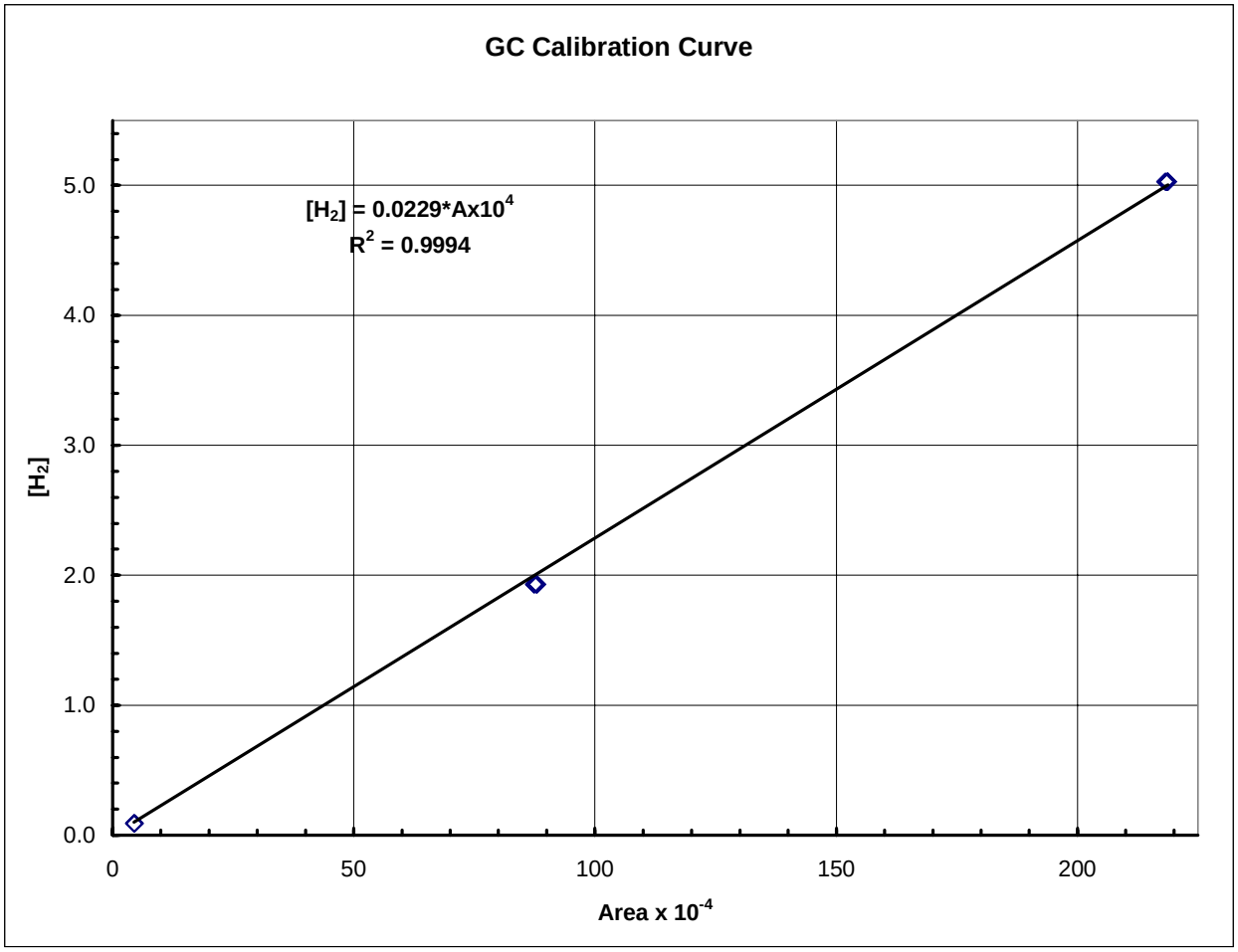


**Figure 11 GC calibration curve example.**

The GC control, data collection, and data analysis was conducted online using software provided by CHROM Perfect.

## 3.3 Experimental Procedure

The procedure adopted for the high-pressure, high-temperature inorganic hydrogen membrane permeation testing was conducted in a step-wise fashion. An example of the test procedure is illustrated in Figure 12.

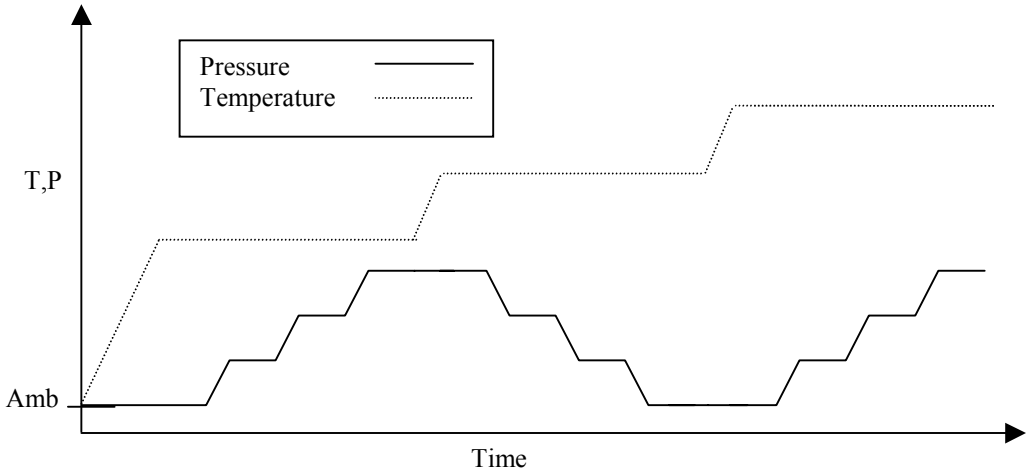


**Figure 12 Schematic of the hydrogen membrane testing procedure.**

The initial temperature ramp of the HMT unit was conducted under argon gas on the sweep side and helium on the retentate side of the membrane. Helium was chosen for the heat-up gas and was used as a tool for the detection of existent or newly developed leaks in the membrane as a result of thermal stresses. After the desired test temperature was attained, the process gas mixture, which was a known composition of $H_2$/He or $H_2/N_2$, was introduced to the retentate side of the membrane. It should be noted that ample time was given to allow the system to equilibrate with respect to pressure, temperature and gas changes, which was monitored with the use of the GC. Test samples were taken every ten minutes for a duration that allowed for an ample number of GC measurements at each test condition. The test parameters that were recorded at every reading were room temperature and pressure, sweep flow rate and pressure, feed flow rate and pressure, membrane temperature, and the hydrogen concentration measured by the GC.

## 4.0 CALCULATION OF MEMBRANE CHARACTERISTICS

Hydrogen transport through dense materials has been of interest since its discovery in the 1860's by researchers such as Deville, Graham and Troost (Grashoff et al. 1983). The hydrogen transport through dense cermet and metal membranes is described by ionic- or atomic-transport. The mechanism associated with ionic- and atomic-hydrogen transport is described below (Hsieh, 1996):

1) Transport of hydrogen from the bulk gas to membrane surface.
2) Chemisorption of the hydrogen molecules on the membrane surface.
3) Dissociation of the hydrogen molecule:
    a) Into two hydrogen atoms (atomic transport).
    b) Into hydrogen protons and electrons (ion transport).
4) Ionic- or atomic-diffusion of the dissolved hydrogen in the membrane in the direction of decreasing hydrogen concentration.
5) Recombination of the hydrogen atoms or the hydrogen protons and electrons.
6) Desorption of combined hydrogen molecules.
7) Transport of hydrogen from membrane surface to bulk gas.

The above mechanism describing ionic- and atomic-diffusion is illustrated in Figure 13 (Hsieh, 1996).

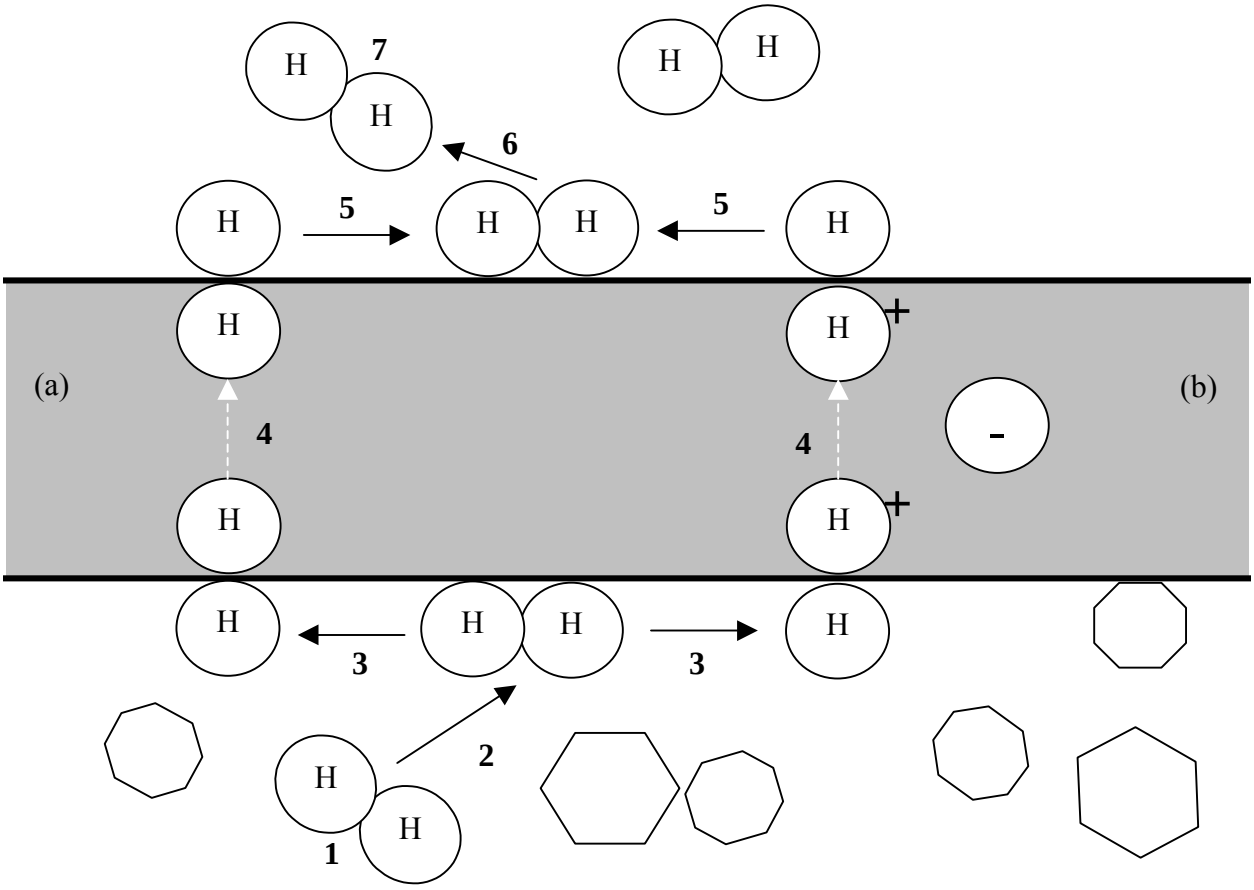


**Figure 13 Transport mechanism of hydrogen through dense membrane materials. (a) Atomic-diffusion. (b) Ionic-Diffusion.**

## 4.1 Derivation of Governing Permeation Equation

Fick's law, equation (4-1), defines the transient mass transfer of species A in the direction of decreasing concentration of A.

$$\frac{dN}{dt} = -D\frac{dC}{dx} \tag{4-1}$$

In the relation to the hydrogen membrane processes, the direction of mass transfer would be defined from the retentate (hydrogen rich feed stream) to the permeate (hydrogen poor stream). Assuming a steady state permeation process and integrating Equation (4-1) yields the

governing, steady state form of Fick's law for membrane processes (Perry's Chemical Engineer's Handbook, 1984).

$$N_H = 2N_{H_2} = -D_M \frac{\Delta C_H}{t_M} \tag{4-2}$$

Where $N_H$ is the atomic flux of hydrogen, $N_{H2}$ is the molecular flux of hydrogen, $D_M$ is the diffusivity of the membrane material, $\Delta C_H$ is the atomic concentration gradient across the membrane thickness, $t_M$.

The rate-limiting step in the membrane mechanism is sought to be the diffusion of the hydrogen through the membrane, because of the rapid dissociation of the hydrogen molecules on the membrane surface. As a result of the slow diffusion process, it can be assumed that the atomic concentrations at the membrane surfaces are at equilibrium with the retentate and permeate hydrogen gases. Application of Sieverts thermodynamic relation (Sievert et al.,), equation (4-3), gives the atomic concentration of hydrogen in terms of the partial pressure of the hydrogen gas at the membrane surface.

$$C_H = K_S P_{H_2}^{0.5} \tag{4-3}$$

Combining equations (4-2) and (4-3) gives the governing membrane permeation equation in terms of the hydrogen partial pressures of the retentate and permeate, the Richardson Equation, (4-4), as proposed by Buxbaum and Marker, 1993.

$$N_{H_2} = -\frac{D_M K_S}{2} \frac{\left(P_{H_2,Ret}^{0.5} - P_{H_2,Per}^{0.5}\right)}{t_M} \tag{4-4}$$

Defining the isothermal permeability constant of a membrane material by half of the product of the membrane diffusivity and the Sieverts constant and substituting into the Richardson Equation, (4-5), yields Equation (4-6), which is the governing equation for membrane processes with atomic- or ionic-transport mechanisms.

$$N_{H_2} = -k_M \frac{\left(P_{H_2,Ret}^{0.5} - P_{H_2,Per}^{0.5}\right)}{t_M} \tag{4-5}$$

The rate of the molecular dissociation on the membrane surface and atomic-diffusion through the membrane has a large influence on the exponent of the partial pressure drop across the membrane. If dissociation of the membrane mechanism is the rate-limiting step, then the exponent of the partial pressure is 1.0. While, membranes whose mechanism is governed by a rate-limiting step of diffusion have an exponent of 0.5 on the partial pressure expression. However, it has been established that for some atomic- or ionic-diffusion processes it is not uncommon to experience exponents ranging form 0.5 to 1.0 due to the competing rates of dissociation and diffusion (Hurlbert et al. 1961). Thus, equation (4-6) represents a more generic form of the membrane governing equation, which compensates for the competing "rate-determining steps" associated with the applicable mechanism.

$$N_{H_2} = -k_M \frac{\left(P_{H_2,Ret}^{n} - P_{H_2,Per}^{n}\right)}{t_M} \text{ or } R_{H_2} = -\frac{k_M A_M}{t_M}\left(P_{H_2,Ret}^{n} - P_{H_2,Per}^{n}\right) \tag{4-6}$$

## 4.2 Application of the Governing Permeation Equation

The governing equation, (4-6), used for membrane evaluation is illustrated in the previous section. As a result of a high sweep flow rate and a low permeation rate through the membrane, the partial pressure of hydrogen on the permeate side of the membrane was assumed to be negligible. As a result of this simplification, equation (4-6) reduced to

$$N_{H_2} = -k_M \frac{P^n_{H_2,Ret}}{t_M} \quad \text{or} \quad R_{H_2} = -\frac{k_M A_M}{t_M} P^n_{H_2,Ret} \tag{4-7}$$

The unknowns in Equation (4-7), the partial pressure exponent and the membrane's permeability constant can be calculated from a log-log plot of the hydrogen partial pressure of the retentate versus the rate of hydrogen transport through the membrane. The hydrogen rate was obtained by application of the collected data to Equation (4-8).

$$R_{H_2} = y_{H_2,Per} Q_{Per\,(STP)} \tag{4-8}$$

An example of the resultant plot is illustrated in Figure 14, where the data is "best-fit" to a linear relationship.

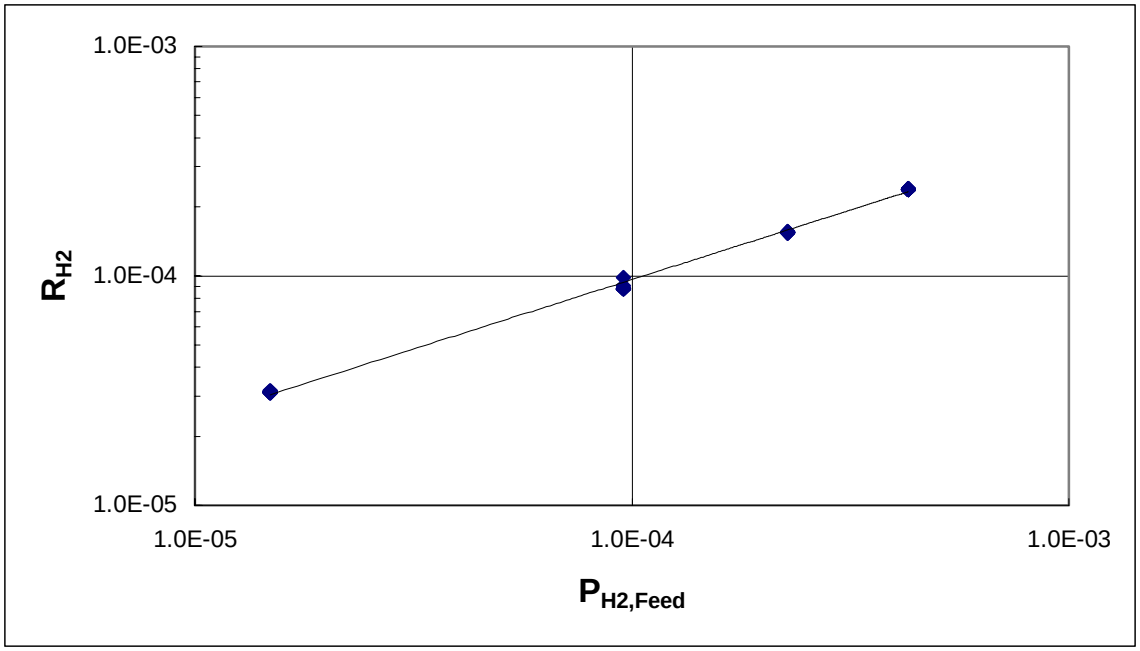


**Figure 14 Example of the log-log plot in the determination of the membrane characteristics.**

The isothermal permeability constant and the partial pressure exponent can be calculated from the intercept, b, and the slope, m, of the example graph in Figure 14 by the following relations.

$$b = \log \frac{k_M A_M}{t_M} \tag{4-9}$$

$$m = n \tag{4-10}$$

An example calculation of the permeability can be found in Appendix A.

### 4.3 Temperature Dependence of the Membrane Permeability

The hydrogen permeability of a membrane material is a function of temperature and can be described by an Arrenhius-type relation, Equation (4-11).

$$k_P = k_o \exp\left(\frac{-E_P}{RT}\right) \tag{4-11}$$

Where $k_P$ is the membrane permeability, $k_o$ is the pre-exponential permeability constant, $E_P$ is the activation energy for permeation and R and T are the gas constant and absolute temperature, respectively. An example of the temperature dependence of permeability calculation can be found in Appendix A.

## 5.0 RESULTS AND DISCUSSION

The experiments were conducted at the NETL's Hydrogen Membrane Technology facility to determine the hydrogen permeability through palladium, tantalum Inconel 600, and a cermet membrane. The membrane permeability constant ($k_P$) and partial pressure exponent (n) were calculated using the method described in Section 4. The isothermal results of the high-pressure, high-temperature hydrogen membrane testing are summarized in Table 3. The membrane permeability constant, $k_P$, is illustrated in Table 3 using two methods. The first is by calculating the permeability and exponent simultaneously from the experimental data. In this study, the partial pressure exponent was found to vary from 0.4 to 0.75, which is comparable with the literature findings of Hurlbert et al. 1999. As a result of the permeability value being a strong function of the exponential value, membranes cannot be contrasted by simply comparing their permeability.

The second method of calculating the characteristics of dense hydrogen membranes was by setting the partial pressure exponent, n, to be 0.5 and then solving for the permeability. Equating the exponent to 0.5 is associated with the assumption that hydrogen diffusion is the rate-limiting step in the membrane's mechanism. Therefore, equating the partial pressure exponent to 0.5 allows a basis for comparison of membrane permeability from several studies, although more accurate descriptions of the membranes overall behavior are obtained by optimizing both the exponent and the permeability.

**Table 3 Summary of the hydrogen permeability experiments conducted at the NETL.**

| Membrane Composition | $t_M$ (mm) | T (K) | n | k (mol $H_2$/m s $Pa^n$) | k′ (mol $H_2$/m s $Pa^{0.5}$) |
|---|---|---|---|---|---|
| Palladium #1 | 1.0 | 623 | 0.62 | $2.23x10^{-9}$ | $1.47x10^{-8}$ |
| Palladium #1 | 1.0 | 723 | 0.61 | $4.15x10^{-9}$ | $2.20x10^{-8}$ |
| Palladium #1 | 1.0 | 908 | 0.55 | $1.38x10^{-8}$ | $3.30x10^{-8}$ |
| Palladium #1 | 1.0 | 1038 | 0.57 | $1.73x10^{-8}$ | $5.23x10^{-8}$ |
| Palladium #1 | 1.0 | 1173 | 0.57 | $2.28x10^{-8}$ | $6.84x10^{-8}$ |
| Palladium #2 | 0.8 | 623 | 0.74 | $2.88x10^{-10}$ | $1.19x10^{-8}$ |
| Palladium #2 | 0.8 | 723 | 0.70 | $6.94x10^{-10}$ | $1.60x10^{-8}$ |
| Palladium #2 | 0.8 | 908 | 0.71 | $9.55x10^{-10}$ | $2.60x10^{-8}$ |
| Palladium #3 | 1.0 | 908 | 0.61 | $6.76x10^{-9}$ | $3.87x10^{-8}$ |
| Tantalum #2 | 1.0 | 873 | 0.44 | $1.78x10^{-8}$ | $9.12x10^{-9}$ |
| Tantalum #1 | 1.0 | 973 | 0.68 | $1.54x10^{-9}$ | $2.19x10^{-8}$ |
| Tantalum #1 | 1.0 | 1073 | 0.55 | $8.99x10^{-9}$ | $1.38x10^{-8}$ |
| Tantalum #1 | 1.0 | 1173 | 0.57 | $6.88x10^{-9}$ | $1.97x10^{-8}$ |
| ANL-1,#7 | 1.2 | 973 | 0.55 | $8.00x10^{-9}$ | $6.77x10^{-9}$ |
| ANL-1,#6 | 1.2 | 1073 | 0.53 | $7.22x10^{-9}$ | $1.13x10^{-8}$ |
| ANL-1,#5 | 1.2 | 1173 | 0.51 | $4.98x10^{-9}$ | $1.71x10^{-8}$ |
| Inconel 600 | 1.1 | 873 | 0.62 | $1.04x10^{-11}$ | $6.38x10^{-11}$ |
| Inconel 600 | 1.1 | 973 | 0.60 | $2.77x10^{-11}$ | $1.42x10^{-10}$ |
| Inconel 600 | 1.1 | 1073 | 0.51 | $2.82x10^{-10}$ | $3.37x10^{-10}$ |
| Inconel 600 | 1.1 | 1173 | 0.48 | $8.08x10^{-10}$ | $4.92x10^{-10}$ |

### 5.1 Palladium Membrane

Three palladium membrane samples, palladium #1, palladium #2 and palladium #3, were studied as a reference material for the verification of the operation and validation of the HMT unit. The palladium #1 sample was tested at pressure and temperature ranges of 101 to 2757kPa and 623 to 1173 K, respectively. The high-pressure, high-temperature evaluation of the palladium #1 exhibited good results as compared to the literature values of Koffler (1969) when it is depicted as a function of temperature in Figure 20.

The permeability experiments of the palladium #2 membrane, were conducted at pressure and temperature ranges of 101 to 2757kPa and 623 to 908 K, respectively. The initial

permeability results of palladium #2 yielded a value quite higher than that of Koffler (1969). The reason for this high permeation with sample #2 was attributed to the observed deformation of the 1mm-thick palladium disk under the test conditions. The palladium sample "bowed" out due to the pressure differential across the membrane, causing palladium #2 to yield. This deformation increased the permeation rate of hydrogen through the bulk metal for two reasons. First, because the geometry of the membrane changed from a flat disk to a portion of a hemisphere, thereby increasing the surface area for hydrogen permeation. Secondly, because the mass of the membrane was constant, the thickness of the membrane would have had to decrease to allow for the increase in surface area. This also served to facilitate hydrogen transport.

Since the rate of deflection of the membrane during testing could not to be measured as a function of time, it was assumed that the membrane was deflected upon initial heat-up of the HMT unit. Therefore, the palladium #2 results for permeability were based on the final thickness and area of the membrane.

After inspection of the first palladium membrane, it was concluded that palladium #1 did not experience any distortion because of the position of the sweepside concentric tube and thermocouple with respect to the membrane. The concentric tube and thermocouple were placed close enough to the surface of the membrane for them to act as a support, preventing the deflection of the sample. This was evidenced during the inspection of the palladium #1 sample by an impression of the concentric tube and thermocouple on the center of the palladium disk.

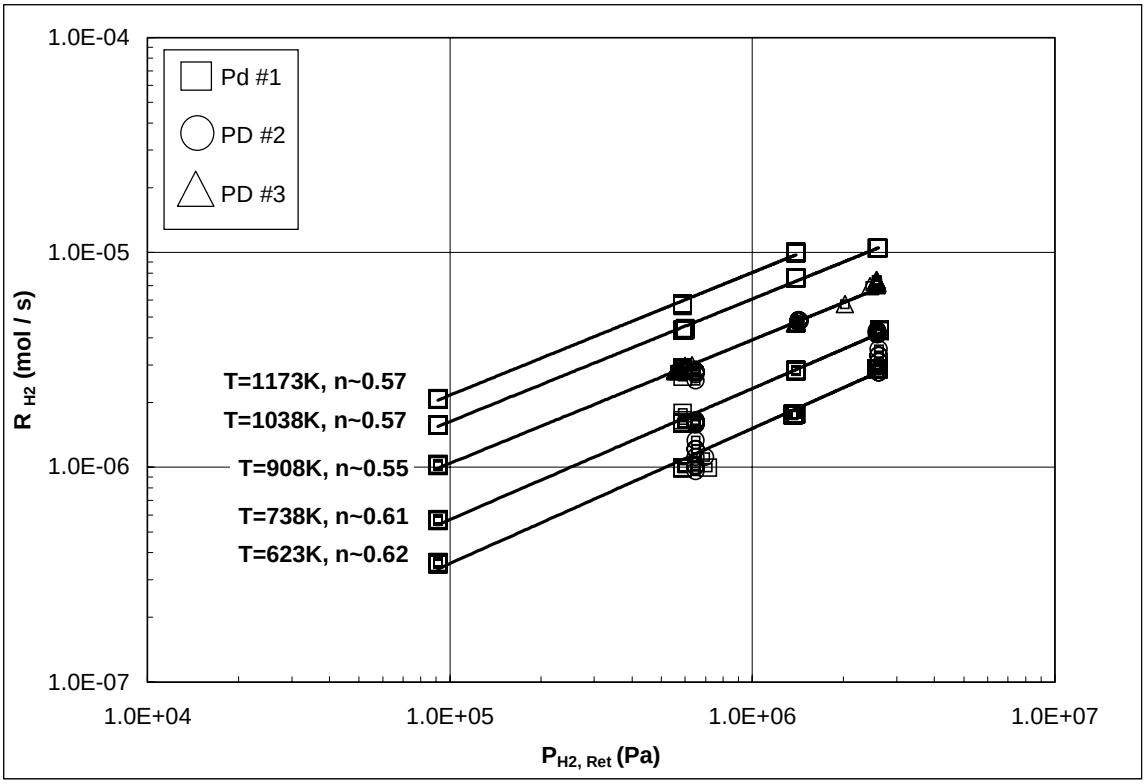


**Figure 15 Isothermal permeance data for bulk palladium.**

The palladium #3 experiments were conducted at a pressure range similar to the previous samples, 101 to 2757kPa, while the temperature of this membrane experiment was kept at 908 K. The results obtained form the experiments on the palladium #3 sample were in good agreement with the palladium #1 sample and thus in good agreement with the literature values of Koffler (1969). The mechanical integrity of the palladium #3 sample was maintained by the placement of the concentric sweepside tubes close enough to the membrane surface to act as a support and prevent deformation.

A comparison between the isothermal behavior of the palladium membrane samples is illustrated in Figure 15 and Table 3. This plot was used to determine the exponent and permeability constant that best fit the palladium data.

## 5.2 ANL-1 Cermet Membrane

Three cermet membrane tested in this study were fabricated by Argonne National Laboratory. The isothermal membrane characteristics of the ANL-1 membranes are summarized in Table 3 and illustrated in Figure 16.

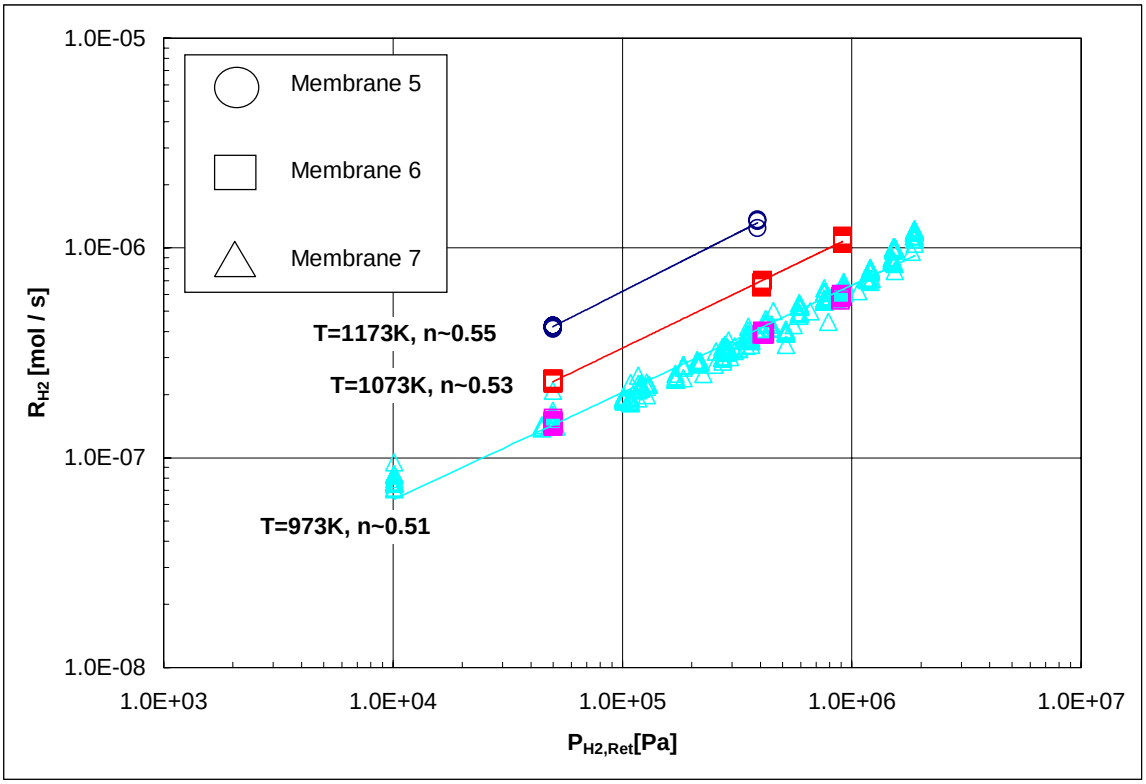


**Figure 16 Isothermal permeation data for the cermet membrane ANL-1.**

Although the ANL-1 cermet membrane is composed of 40% nickel by volume, the hydrogen permeation rate was much higher than that initially expected. The cermet membranes permeation rate was roughly one order of magnitude less than the palladium membranes tested at low temperatures (~873K).

Although the permeability data shown by the ANL-1 cermet in this study was promising given the relatively low costs of its components, the cermet-to-metal seal remained a concern.

The cermet membrane testing on the three ANL-1 membranes did not last over 70 hours in any case. After visual inspection of the mounted cermet membranes, however, it was determined that the leak occurred from the cermet-to-metal seal.

### 5.3 Inconel 600 Membrane

The HMT unit is primarily constructed of 316 stainless steel which incompatible with the operating conditions in which the HMT unit's "hot-zone". Therefore, the material of construction chosen for this area of the unit was made of Inconel 600. Since most metals are permeable to hydrogen, experiments were needed to quantify the net permeation effect of Inconel 600 on other membrane testing results.

The Inconel 600 membrane was found to be permeable to hydrogen at the HMT's operating conditions. The permeability of the Inconel 600 was two orders of magnitude less when compared to palladium. As a result of the Inconel 600 membrane testing analysis and the geometry of the system, it was assumed that the HMT's construction had negligible impact on the permeation results of the other membranes tested. The Inconel's isothermal permeability results are illustrated in Figure 17 while a comparison between Inconel 600 with other membrane materials is given in Figures 19 and 20 as a function of temperature and Table 5 in Arrhenius plot form.

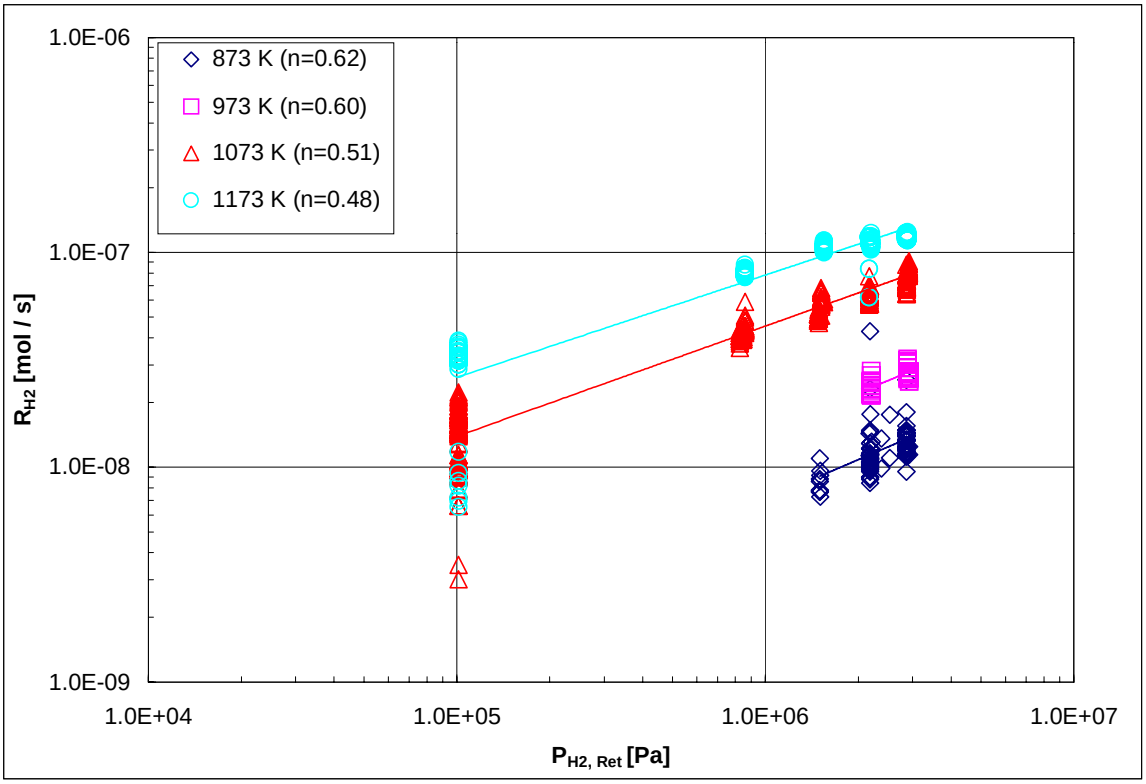


**Figure 17 Isothermal permeability data of bulk Inconel 600.**

## 5.4 Tantalum Membrane

The tantalum membrane tested at the NETL resulted in a permeability roughly of the same order of magnitude as palladium. The isothermal permeability results are summarized in Table 4 and are illustrated in Figure 18.

The permeability of the tantalum membranes was less than expected when compared to the literature values published by Steward (1983). This reference is not based on hydrogen permeation experiments, however, but rather on the product of hydrogen solubility in tantalum and the diffusion constant for the hydrogen-tantalum system. The scatter in the data may be attributed to the formation of tantalum oxides or other contaminats on the surface of the tantalum membrane. These compounds can provide mass transfer resistances or diminish the catalytic activity of the tantalum to dissociate hydrogen.

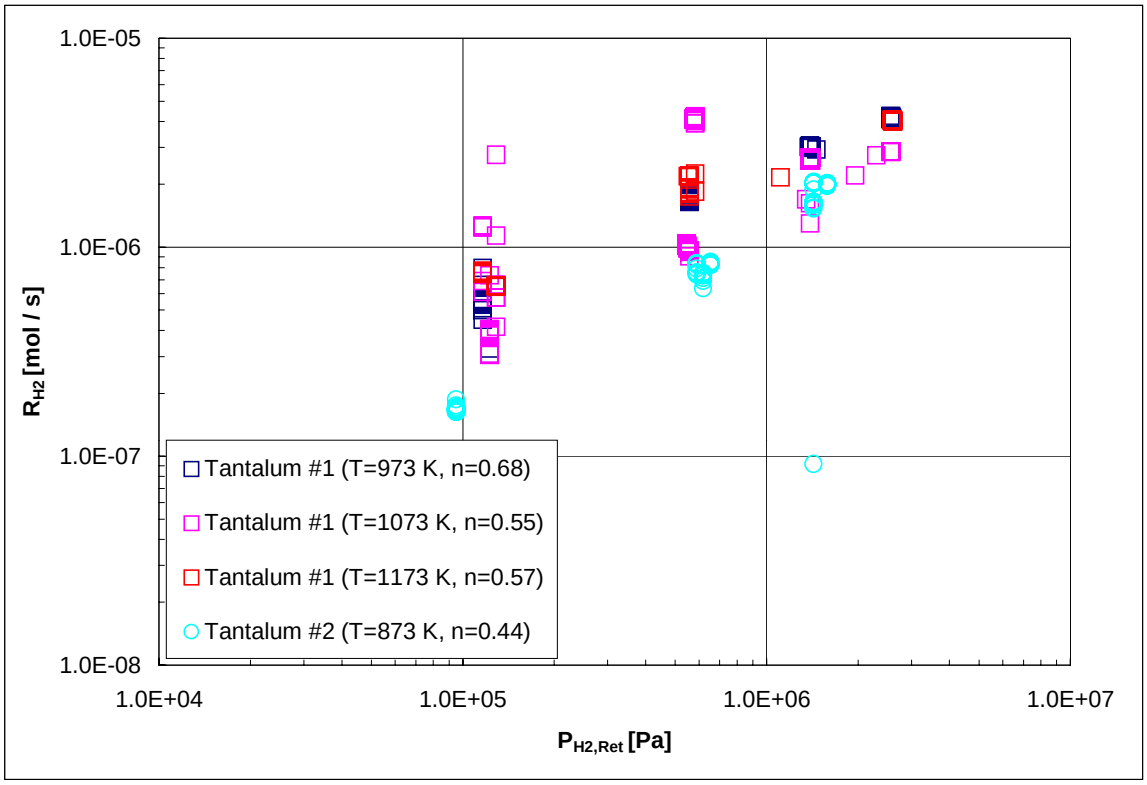


**Figure 18 Isothermal permeability data of bulk tantalum.**

Surface analysis was conducted on the tantalum membrane to validate the difference between the theoretical permeation values and the data obtained in this study. X-ray photoelectron spectroscopy (XPS) surface analysis of a pre-tested tantalum membrane, which had been cleaned with a 40% H2SO4, 20% HNO3 and 20% HF acid mixture by volume, showed a relatively small amount of surface oxides. The surface analysis resulted in a negligible oxygen concentration after about 25 angstroms into the membrane to a high oxygen concentration of 35% at the surface.

It seems that during testing of the tantalum #1 membrane sample, oxygen was unexpectedly introduced to the retentate side of the HMT unit due to complications in the system. The XPS surface analysis of retentate surface of the membrane resulted in oxygen

concentrations of approximately 40% at the surface to relatively steady concentrations levels of about 10% from 460 to 1500 angstroms into the tantalum membrane.

The permeate surface of the membrane was assumed not to have been exposed to any amount of oxygen during the test. The XPS analysis of the surface validated this assumption due to the similarity of the oxygen concentration and depth of oxygen present of the pre- and post-tested membranes.

The surface analysis conducted on the tantalum membrane also resulted in carbon concentrations which were minutely present prior to membrane testing. Carbon concentrations on the tantalum membrane ranged from as high as 60% on the surface to 30% at depths of 1500 angstroms into the membrane. The unexpected high carbon content may be either a result of atmospheric carbon or more likely residual hydrocarbons from the "working" of the metals in the HMT unit.

### 5.5 Membrane Comparison

Figure 19 shows the hydrogen permeabilities of the materials tested in this study as a function of reciprocal of temperature, where the partial pressure exponents varied from 0.4 to 0.75. While, Figure 20 depicts the analysis of the membrane's hydrogen permeability as a function of the square root of the partial pressure, regardless of the "best-fit" value of the partial pressure exponent. The permeabilities illustrated in both Figures 19 and 20 are "best-fit" to an Arrhenius type expression for all of the isothermal permeability data of a given membrane composition. The Arrhenius expression is given in Equation (13) while the proper constants are listed in Table 5.

$$k_P = k_o \exp\left(\frac{-E_P}{RT}\right) \qquad (5\text{-}1)$$

The permeability results in Figure 19 show the change in the partial pressure exponential values of the membranes tested. Although the permeability scatter represented by Figure 19 makes it impractical for comparison with literature permeability, it gives a strong qualitative relationship to the importance and the influence of the partial pressure exponent on the membrane permeability as indication of its mechanistic rates. By equating the exponent to the square root of the hydrogen partial pressure, however, quantitative literature comparisons can be made, as illustrated in Figure 20.

The palladium experiments conducted in this study were in very good agreement with the selected literature values of Koffler (1969) when the partial pressure exponent was forced to 0.5 as depicted in Figure 20. The Arrhenius plot, which was a "best-fit" of the three palladium membranes tested exhibited permeability differences as small as 12% at 738 K, while increasing to a maximum difference 31% at 1173 K when compared with that of Koffler (1969).

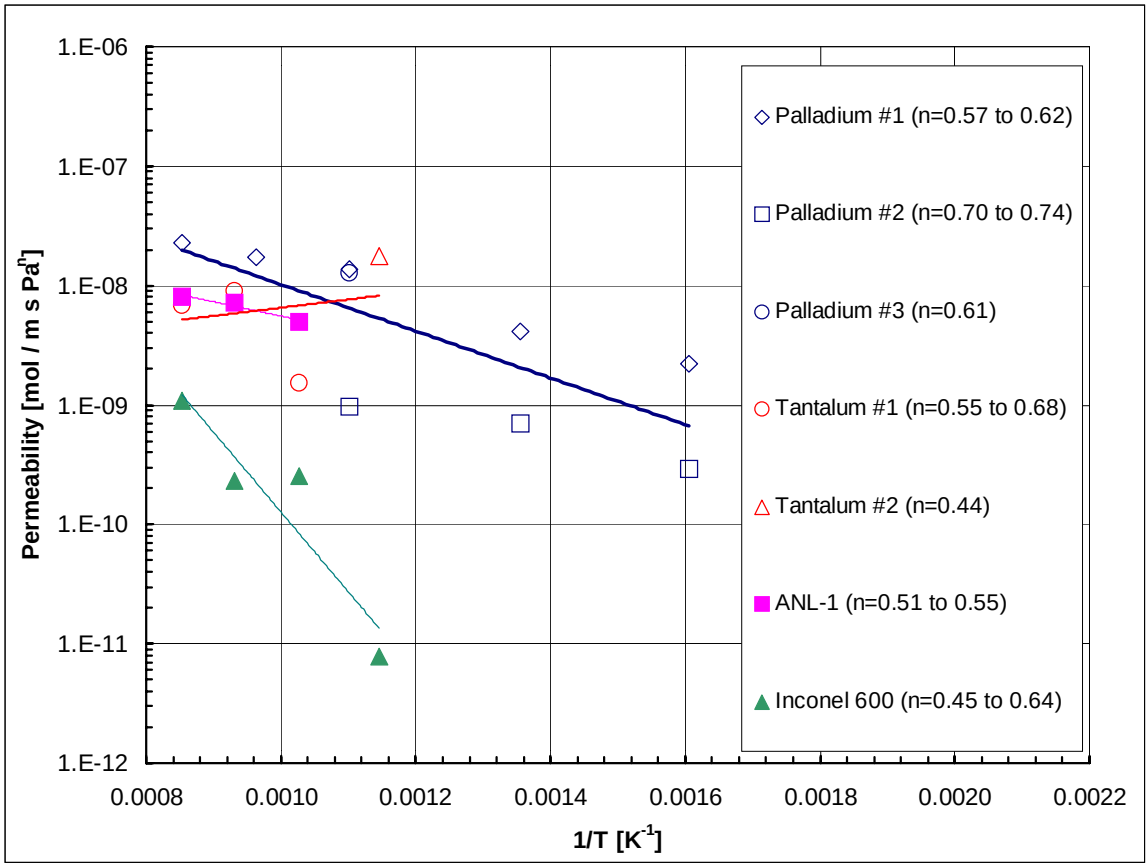


**Figure 19 Permeability results of selected membranes as a function of temperature with different partial pressure exponents.**

The tantalum results obtained were found to dramatically vary from the permeability values reported by Steward (1983). Quantitatively, the "best-fit" Arrhenius permeability results of the two tantalum samples in this study varied from 57% at 1173 K to as much as 88% at 873 K when compared with the data of Steward (1983). Moreover, the slope of the "best-fit" Arrhenius permeability relation was negative in this study, while Steward (1983) reports that the slope of the temperature dependence permeability to be positive. It should be noted however, that the permeability data illustrated by Steward (1983) is a compilation of the solubility and diffusivity work of Veleckis and Edwards (1969). Thus, with no direct quantitative permeation studies of the hydrogen/tantalum system found, comparisons of similar membrane studies are

referenced to the data compiled by Steward (1983). The difference in the slope of the tantalum permeability could be attributed to the increased surface resistance associated with lower temperatures. This indicates that the surface resistances decreases with increasing temperature and the rate of hydrogen dissociation increases with temperature.

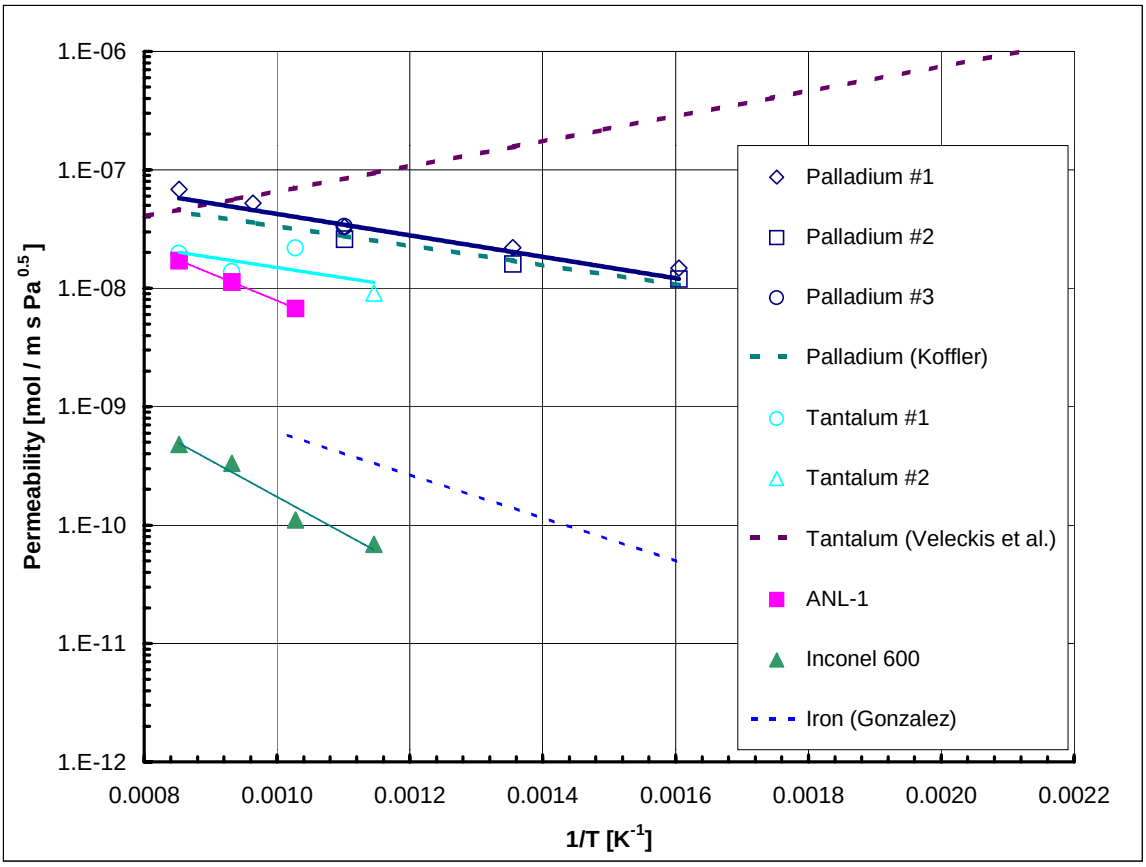


**Figure 20 Permeability results of selected membranes as a function of temperature with a partial pressure exponent forced to 0.5.**

**Table 4 Summary of literature permeation values of palladium and permeation results obtained in this study (DOE).**

| Researcher | Composition | $t_M$ (μm) | T (K) | $P_{TOT,Ret}$ (kPa) | $P_{TOT,Per}$ (kPa) | $P_{H2,Ret}$ (kPa) | $P_{H2,Per}$ (kPa) | $k_O$ (mol $m^{-1}s^{-1}Pa^{-0.5}$) | $E_P$ KJ $mol^{-1}$ |
|---|---|---|---|---|---|---|---|---|---|
| Balavnev et al. 1974 | Pd | 100-1000 | 370-900 | $3x10^{-8}$-$7x10^{-5}$ | 101.3 | $3x10^{-8}$-$7x10^{-5}$ | 101.3 | $1.89x10^{-7}$ | 15.46 |
| Davis et al. 1954 | Pd | 130-729 | 473-973 | $3x10^{-3}$-101 | Vacuum | $3x10^{-3}$-101 | Vacuum | $3.85x10^{-7}$ | 18.56 |
| Holleck et al. 1967 | Pd | 800-2025 | 500-900 | ~53 | 0.024-0.006 | ~53 | 0.024-0.006 | $1.64x10^{-8}$ | 12.82 |
| Hurlber et al. 1961t | Pd | 10-150 | 623-773 | 101-710 | Vacuum | 101-710 | Vacuum | $1.47x10^{-8}$ | 11.92 |
| Katsuta et al. 1979 | Pd | 940 | 769-1219 | 101 | Vacuum | 101 | Vacuum | $3.82x10^{-7}$ | 20.50 |
| Koffler et al. 1969 | Pd | 486-762 | 300-709 | $4x10^{-5}$-$7x10^{-3}$ | $1.3x10^{-8}$ | $4x10^{-5}$-$7x10^{-3}$ | $1.3x10^{-10}$ | $2.20x10^{-7}$ | 15.67 |
| Toda et al. 1958 | Pd | 11500 | 443-563 | ~84 | Vacuum | ~84 | Vacuum | $1.72x10^{-7}$ | 13.46 |
| DOE | Pd | 1000 | 623-1173 | 101-2757 | ~120 | 91-2481 | Ar Sweep | $3.40x10^{-7}$ | 17.29 |

**Table 4 continued…**

| Researcher | Composition | $t_M$ (μm) | T (K) | $P_{TOT,Ret}$ (kPa) | $P_{TOT,Per}$ (kPa) | $P_{H2,Ret}$ (kPa) | $P_{H2,Per}$ (kPa) | $k_O$ (mol $m^{-1}s^{-1}Pa^{-0.5}$) | $E_P$ KJ $mol^{-1}$ |
|---|---|---|---|---|---|---|---|---|---|
| DOE | Inconel 600 | 1000 | 873-1173 | 101-2930 | ~120 | 101-2930 | Ar Sweep | $2.02x10^{-7}$ | 58.70 |
| DOE | ANL-1 | ~1000 | 973-1173 | 101-1125 | ~120 | 91-1013 | Ar Sweep | $1.57x10^{-6}$ | 44.06 |
| DOE | Ta | 1000 | 873-1173 | 101-1125 | ~120 | 91-1013 | Ar Sweep | $1.1x10^{-7}$ | 16.63 |

# 6.0 CONCLUSION

From this study the following conclusions can be drawn:

1. The agreement between the literature and experimental permeability values validates the integrity of the HMT unit to test membranes at high pressures and temperatures.
2. The data also showed that the rate-limiting step in the hydrogen transport mechanism was dependent on the membrane material.
3. The exponents of the hydrogen partial pressures varied from 0.4 to 0.75, which demonstrates that diffusion is not the rate-limiting step in many membrane materials, but rather it is a complex mechanism involving competing surface and diffusion effects.
4. The high-pressure, high-temperature results of the palladium membrane testing demonstrated the high permeability and 100% selectivity to hydrogen, which makes palladium the material of choice for many membrane applications.
5. Of the membranes tested, palladium exhibited the highest catalytic surface due to the rapid equilibration of the hydrogen flux upon changing process conditions as well as the analysis of the partial pressure exponent yielding values near 0.5 in the majority of the experiments.
6. The cermet membrane provided by Argonne National Laboratory showed tremendous promise in hydrogen membrane technology. Although the ANL-1 cermet membrane, which is 40% metallic nickel by volume, exhibited permeation values less than palladium, the results were much higher than those expected due to the membranes nickel composition.

7. The mechanical integrity of the cermet membranes also showed promise during testing.
8. The bulk tantalum membranes tested showed much lower permeation values than the theoretical results illustrated by Steward (1983). The low permeation values obtained were attributed to the high surface resistances associated with the hydrogen transport mechanism (Buxbaum et al. 1993).
9. Although the surface resistances were dominating the hydrogen permeation of the tantalum membrane, the permeation values obtained were roughly on the same order of magnitude as the ANL-1 membrane and one order of magnitude less than the palladium membrane. Thus, the attractiveness of a bulk tantalum membrane is very low as a result of the strong formation of oxides on the membrane surface and hence an increased surface resistance to hydrogen permeation.
10. The high temperature, high pressure hydrogen membrane testing demonstrated the temperature and pressure dependence of the tested materials as that reported at lower conditions.

# 7.0 RECOMMENDATIONS

The following recommendations are proposed in order to further develop and understand the hydrogen – dense membrane system.

1. Uncouple the mechanistic rates associated with the surface and the diffusion processes.
2. Conduct experiments to study the effects of oxygen contamination on bulk tantalum hydrogen transport.
3. Expand the scope of hydrogen membrane materials (ex. V, Nb, Zr, etc.).
4. Synthesize composite hydrogen membranes utilizing materials that exhibit high diffusion and dissociation characteristics for substrate and film applications.
5. Further develop the effectiveness of cermet membranes by application of different metals and oxides.
6. Address longevity problem with respect to the metal-to-ceramic seal.
7. The cost, performance, or applicability of materials however, requires more research to advance high-pressure, high-temperature, inorganic membrane technology.

# APPENDIX

# APPENDIX A

## Sample Calculation of the Isothermal Permeability

### *A. Solving for n and $k_P$ simultaneously.*

1. Assumptions

   2. The membrane surface is smooth.

   3. The hydrogen partial pressure on the permeate side of the membrane is very small in comparison with the retentate side, therefore is negligible.

4. The governing equation for hydrogen permeation through dense media is given in terms of hydrogen flux, $N_{H2}$, and rate of hydrogen transport through the membrane, $R_{H2}$, by the following relations respectively.

$$N_{H_2} = -k_M \frac{P_{H_2,Ret}^n}{t_M} \quad \text{or} \quad R_{H_2} = -k_M A_M \frac{P_{H_2,Ret}^n}{t_M}$$

5. The following table illustrates an example of one data set collected under steady state conditions, for an array of given temperatures.

| $y_{H2}$ in Process Gas | Membrane Temperature | Process Gas Flow Rate | Process Gas Pressure | Sweep Gas Flow Rate | Sweep Gas Pressure | $y_{H2}$ in Sweep Gas |
|---|---|---|---|---|---|---|
| | (K) | (smm) | (kPa) | (smm) | (kPa) | |
| 0.90 | 738 | 1.9E-4 | 101.35 | 8.5E-5 | 116.52 | 0.009009 |
| 0.90 | 738 | 1.9E-4 | 652.93 | 8.5E-5 | 116.52 | 0.024649 |
| 0.90 | 738 | 1.9E-4 | 1549.25 | 8.5E-5 | 116.52 | 0.042609 |
| 0.90 | 738 | 1.9E-4 | 2928.20 | 8.5E-5 | 116.52 | 0.063893 |

6. The area of the membrane is calculated using the inside diameter of the membrane holder (0.51 inches).

$$A_M = \frac{\pi D^2}{4} = \frac{\pi (0.51\text{in})^2}{4} * \frac{(2.54\text{cm})^2}{\text{in}^2} = 1.317\text{cm}^2 = 1.317\text{x}10^{-4}\,\text{m}^2$$

7. Calculation the hydrogen partial pressures of the process gas feed.

$$p_{H2,Ret} = y_{H2,Ret} P_{Ret} = (0.90)(101.35\,\text{kPa}) = 91.21\,\text{kPa}$$

8. The rate of hydrogen passing through the membrane is then calculated

$$R_{H_2} = \frac{Q_{Sweep} y_{H2,Per}}{y_{Ar,Per}} * \frac{\text{mol}}{2.24\text{x}10^{-2}\,\text{m}^3} \Rightarrow \frac{\left(85\frac{\text{cm}^3\,\text{Ar}}{\text{min}}\right)_{STP}(0.009009\,\text{mol}\,H_2)}{(1-0.009009)\text{mol Ar}} * \left(\frac{\text{mol Ar}}{22400\text{cm}^3\,\text{Ar}}\right)_{STP}$$

$$R_{H_2} = 3.40\text{x}10^{-5}\,\frac{\text{mol}\,H_2}{\text{min}} = 5.56\text{x}107\,\frac{\text{mol}\,H_2}{\text{s}}$$

9. Calculation of the membrane permeation characteristics is accomplished by first taking the log of the permeation governing equation as follows.

$$R_{H_2} = \frac{k_M A_M}{t_M}\left(P^n_{H_2,Ret} - P^n_{H_2,Per}\right) \Rightarrow R_{H_2} = \frac{k_M A_M}{t_M}\left(P^n_{H_2,Ret}\right) \Rightarrow$$

$$\log R_{H_2} = n \log P_{H_2,Ret} + \log \frac{k_M A_M}{t_M}$$

10. Therefore, the only unknowns in the permeation governing equation are the partial pressure exponent, n, and the membrane permeability $k_P$. The log calculations needed for the analysis of n and $k_P$ are give in the following table.

| $y_{H2}$ in Process Gas | Process Gas Pressure | $y_{H2}$ in Sweep Gas | $p_{H2,Ret}$ | $R_{H2}$ | log $p_{H2,Ret}$ | log $R_{H2}$ |
|---|---|---|---|---|---|---|
| | (kPa) | | (kPa) | (mol $H_2$/s) | (kPa) | (mol $H_2$/s) |
| 0.90 | 101.35 | 0.09009 | 91.22 | 5.67E-7 | 1.96 | -6.25 |
| 0.90 | 652.93 | 0.024649 | 587.64 | 1.62E-6 | 2.77 | -5.79 |
| 0.90 | 1549.25 | 0.042609 | 1394.33 | 2.82E-6 | 3.14 | -5.55 |
| 0.90 | 2928.20 | 0.063893 | 2653.38 | 4.34E-6 | 3.42 | -5.36 |

11. An example of the log of the retentate hydrogen partial pressure, $p_{H2,Ret}$, plotted against the log of the rate of hydrogen transport through the membrane, $R_{H2}$, is shown below.

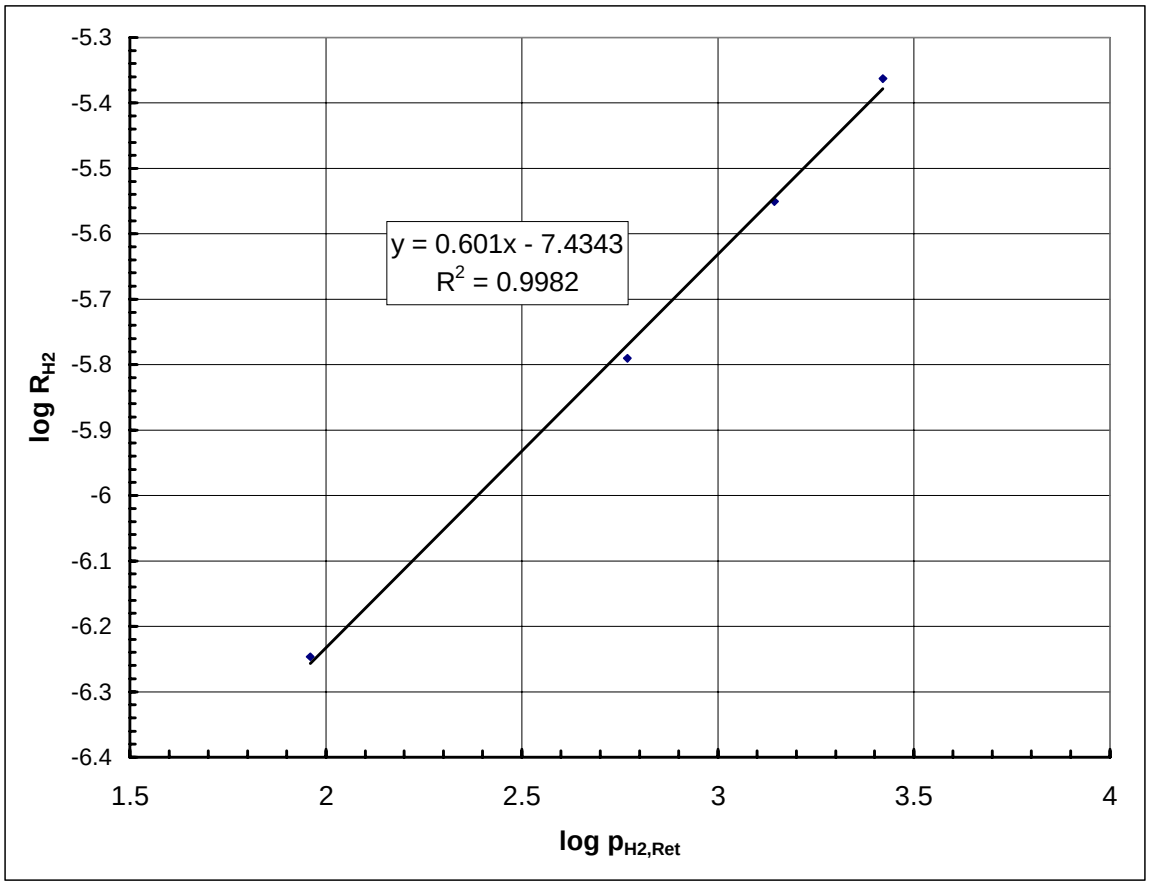


12. Thus, n and $k_P$ are obtaind for the slope and intercept by the following relationships respectively:

$$m = n \therefore n = 0.60$$

and

$$b = \log\frac{k_M A_M}{t_M} \Rightarrow k_M = \frac{t_M}{A_M}10^b = \frac{0.001\,m}{1.317x10^{-4}\,m^2}10^{(-7.4343)}$$

$$k_M = 2.79x10^{-7}\,\frac{mol}{m\,s\,kPa^{1-0.60}} = 1.77x10^{-8}\,\frac{mol}{m\,s\,Pa^{0.40}}$$

***B. Solving for $k_P$ assuming that the rate-limiting step is diffusion (n=0.5).***

5 Assumptions

13. The membrane surface is smooth.
14. The hydrogen partial pressure on the permeate side of the membrane is very small in comparison with the retentate side, therefore is negligible.

6 The governing equation for hydrogen permeation through dense media is given in terms of hydrogen flux, $N_{H2}$, and rate of hydrogen transport through the membrane, $R_{H2}$, by the following relations respectively.

$$N_{H_2} = -k_M \frac{P_{H_2,Ret}^n}{t_M} \quad \text{or} \quad R_{H_2} = -k_M A_M \frac{P_{H_2,Ret}^n}{t_M}$$

7 The following table illustrates an example of one data set collected under steady state conditions, for an array of given temperatures.

| $y_{H2}$ in Process Gas | Membrane Temperature | Process Gas Flow Rate | Process Gas Pressure | Sweep Gas Flow Rate | Sweep Gas Pressure | $y_{H2}$ in Sweep Gas |
|---|---|---|---|---|---|---|
| | (K) | (smm) | (kPa) | (smm) | (kPa) | |
| 0.90 | 738 | 1.9E-4 | 101.35 | 8.5E-5 | 116.52 | 0.009009 |
| 0.90 | 738 | 1.9E-4 | 652.93 | 8.5E-5 | 116.52 | 0.024649 |
| 0.90 | 738 | 1.9E-4 | 1549.25 | 8.5E-5 | 116.52 | 0.042609 |
| 0.90 | 738 | 1.9E-4 | 2928.20 | 8.5E-5 | 116.52 | 0.063893 |

8 The area of the membrane is calculated using the inside diameter of the membrane holder (0.51 inches).

$$A_M = \frac{\pi D^2}{4} = \frac{\pi (0.51\text{in})^2}{4} * \frac{(2.54\text{cm})^2}{\text{in}^2} = 1.317\text{cm}^2 = 1.317\text{x}10^{-4}\,\text{m}^2$$

9 Calculation the hydrogen partial pressures of the process gas feed.

$$p_{H2,Ret} = y_{H2,Ret} P_{Ret} = (0.90)(101.35\,kPa) = 91.21\,kPa$$

10 The rate of hydrogen passing through the membrane is then calculated

$$R_{H_2} = \frac{Q_{Sweep}\, y_{H2,Per}}{y_{Ar,Per}} * \frac{mol}{2.24x10^{-2}\,m^3} \Rightarrow$$

$$R_{H_2} = \frac{\left(85 \frac{cm^3\ Ar}{min}\right)_{STP} (0.009009\ mol\ H_2)}{(1 - 0.009009) mol\ Ar} * \left(\frac{mol\ Ar}{22400 cm^3\ Ar}\right)_{STP}$$

$$R_{H_2} = 3.40x10^{-5} \frac{mol\,H_2}{min} = 5.56x107 \frac{mol\,H_2}{s}$$

11 Calculation of the membrane permeation characteristics is accomplished by solving the rate equation illustrated below.

$$R_{H_2} = \frac{k_M A_M}{t_M}\left(P^n_{H_2,Ret} - P^n_{H_2,Per}\right) \Rightarrow R_{H_2} = \frac{k_M A_M}{t_M}\left(P^n_{H_2,Ret}\right) \Rightarrow$$

$$R_{H_2} = \frac{k_M A_M}{t_M}\left(P^{0.5}_{H_2,Ret}\right)$$

8. Therefore, the only unknown in the permeation governing equation is the membrane permeability constant $k_P$. Sample values of the membrane permeability constant at various temperatures is illustrated in the table below.

| $y_{H2}$ in Process Gas | Process Gas Pressure | $y_{H2}$ in Sweep Gas | $p_{H2,Ret}$ | $R_{H2}$ | $k_P$ |
|---|---|---|---|---|---|
| | (kPa) | | (kPa) | (mol $H_2$/s) | (mol $H_2$ / m s $Pa^{0.5}$) |
| 0.90 | 101.35 | 0.09009 | 91.22 | 5.67E-7 | 1.43E-8 |
| 0.90 | 652.93 | 0.024649 | 587.64 | 1.62E-6 | 1.60E-8 |
| 0.90 | 1549.25 | 0.042609 | 1394.33 | 2.82E-6 | 1.81E-8 |
| 0.90 | 2928.20 | 0.063893 | 2653.38 | 4.34E-6 | 2.02E-8 |

### *C. Solving for the Membrane Permeability as a Function of Temperature.*

The membrane permeability of a species is known to be a function of temperature and can be expressed by an Arrhenius relationship (Perry's Chemical Engineer's Handbook, 1984). The relationship between the membrane permeability and the membrane temperature can be obtained by the construction of a plot of the permeability and the inverse of the absolute temperature. The plot below depicts an example of the permeability and temperature data obtained from a membrane test.

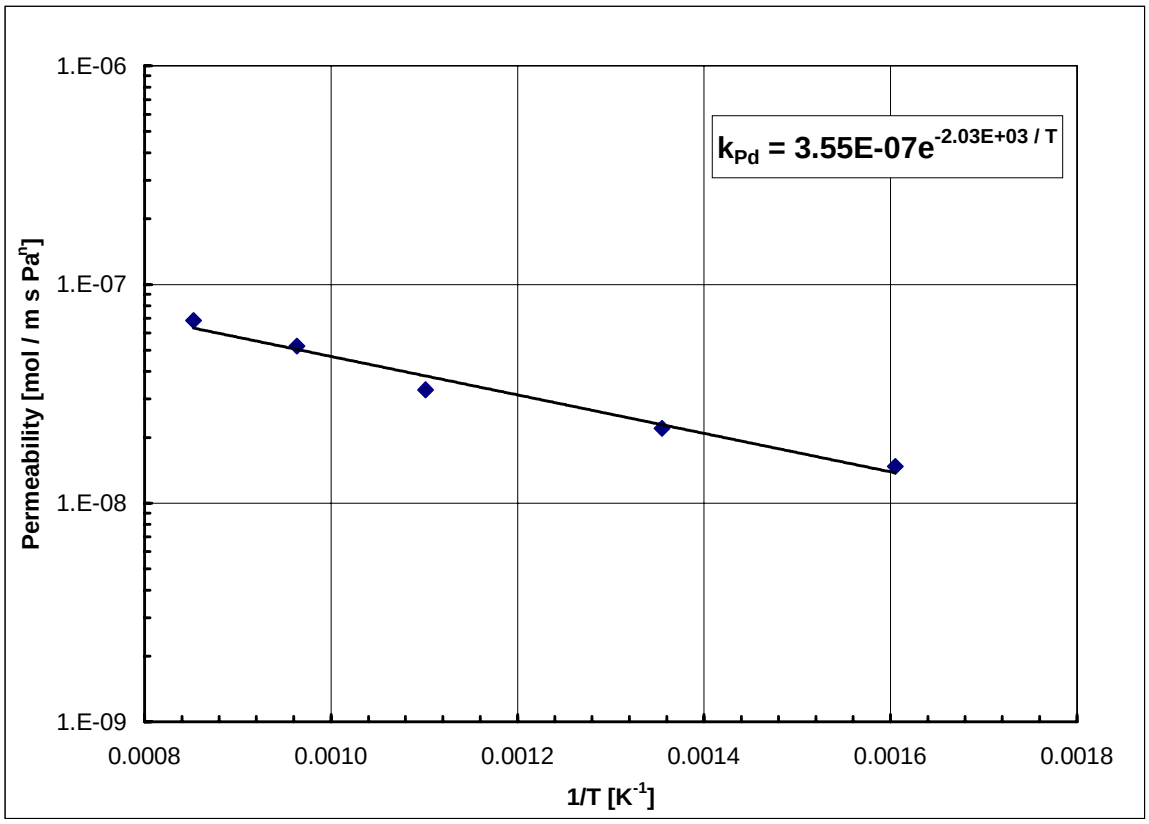


Fitting the data to a "best-fit" relationship gives the pre-exponential factor and the product of the activation energy and the inverse of the universal gas constant. The Arrhenius

relation enables one to calculate the membranes permeability at any temperature within the temperature range of the experiments.

# BIBLIOGRAPHY

## BIBLIOGRAPHY


1. Adris, A.; Lim, C.; Grace, J.; The Fluidized Bed Membrane Reactor System: A Pilot-Scale Experimental Study; Chemical Engineering Science 49, No. 24B (1994) 5833-5843.

2. Armor, J.; Membrane Catalysis: Where Is It Now, What Needs to be Done?; Catalysis Today 25 (1995) 199-207.

3. Balachandran, U.; Guan, J.; Dorris, S. E.; Liu, M.; Development of Proton-Conducting Membranes for Separating hydrogen from Gas Mixtures; extended abstract of presentation at the AIChE 1998 Spring Meeting, New Orleans, LA, March 8-12, 1998.

4. Balovnev, Y.A.; "Diffusion of Hydrogen in Palladium at Low Pressure," Russian Journal of Physical Chemistry 43 No. 10 (1969) 1382-1384

5. Balovnev, Y.A.; "Diffusion of Hydrogen in Palladium," Russian Journal of Physical Chemistry 48 No. 3 (1974) 409-410

6. Barbieri, G,; Violante, V.; DiMaio, F.; Criscuoli, A.; Drioli, E.; Methane Steam reforming Analysis in a Palladium-Based Catalytic Membrane Reactor; Ind. Eng. Chem. Res. 36 (1997) 3369-3374.

7. Barbieri, G.; DiMaio, F.; Simulation of the Methane Steam reforming Process in a Catalytic Pd-Membrane Reactor; Ind. Eng. Chem. Res. 36 (1997) 2121-2127.

8. Basile, A.; Drioli, E.; Santella, F.,; Violante, V.; Capannelli, G,; A Study on Catalytic Membrane Reactors for Water Gas Shift Reaction; Gas Separation & Purification 10(1) (1996b) 53-61.

9. Basile, A.;Criscuoli, A.; Santella, F.; Drioli, E.; Membrane Reactor for Water Gas Shift Reaction; Gas Separation and Purification 10(4) (1996a) 243-254.

10. Benson, H. E.; Processing of Gasification Products; Ch. 25 in Chemistry of Coal Utilization, Elliot, M., ed.; John Wiley and Sons; New York, NY, 1981.

11. Buxbaum, R.E.; Hsu, C.Z.; "Measurement of Diffusive and Surface Transport Resistances for Dueterium in Palladium-Coated Zirconium," J. Nucl. Mat. 189 (1992) 183-192.

12. Buxbaum, R.E.; Kinney, A.B.; "Hydrogen Transport through Tubular Membranes of Palladium-Coated Tantalum and Niobium," Ind. Eng. Chem. Res. 35 (1996) 530-537

13. Buxbaum, R.E.; Marker, T.L.; "Hydrogen Transport Through Non-Porous Membranes of Palladium-Coated Niobium, Tantalum and Vanadium," Journal of Membrane Science, 85 (1993) 29-38

14. Collins, J.P.; Way, J.D.; "Preparation and Characterization of a Composite Palladium-Ceramic Membrane," Ind. Eng. Chem. Res. 32 (1993) 3006-3013

15. Combustion Engineering Incorporated; IGCC Repowering Project, Clean Coal II Project, Public Design Report: October 1993, DOE/MC/26308-5036

16. Cugini, A.; Krastman, D.; Lett, R.; Balsone, G.; Development of a Dispersed Iron catalysis for First Stage Coal Liquefaction; Catalysis Today 19 (1994) 395-408.

17. Damle, A.S.; Gangwal, S.K.; Venkataraman, V.K.; A Simple Model for a Water Gas Shift Membrane Reactor; Gas Separation & Purification 8, No. 2 (1994) 101-106.

18. Davis, W.D.; "Diffusion of Gases Through Metals I. Diffusion of Gases Through Palladium," U.S. Atomic Energy Commission Report No. KAPL-1227, October 1, 1954.

19. DeRossett, A.; "Processing Gases at High Pressures, Diffusion of Hydrogen Through Palladium Membranes," Ind. And Eng. Chem. 52 (1960) 525-528.

20. DeRossett, A.J.; Diffusion of Hydrogen Through Palladium Membranes; Ind. Eng. Chem. 52(6) (1960) 525-528.

21. Deville, H. St.-C.; Comptes rendus 59 (1864) 102

22. Deville, H. St.-C.; Troost, L.; Comptes rendus 57 (1863) 965

23. Enick, R.M.; Hill, J.; Cugini, A.V., Rothenberger, K.S.; McIlvried, H.G.; "A Model of a High Temperature, High Pressure Water-Gas Shift Tubular Membrane Reactor", Am. Chem. Soc., Fuel Chem. Div., Prepr. Pap., 44(4), (1999) 919-923.

24. Enick, R.M.; Morreale, B. D.; Hill, J.; Rothenberger, K.S.; Cugini, A.V.; Siriwardane, R.V.; Poston, J.A.; balachandran, U.; Lee, T.H.; Dorris, S.E.; Graham, W.J.; Howard, B.H.; "Evaluation and Modeling of a High Temperature, High Pressure, Hydrogen Separation Membrane for Enhanced Hydrogen Production from the Water-Gas Shift Reaction" Advances in Hydrogen, 93-100, Kluwer Academic/Plenum Publishers, New York (2000).

25. Fain, D. E.; Roettger, G. E.; Coal Gas Cleaning and Purification with Inorganic Membranes; Trans. of the ASME Journal of Engineering for Gas Turbines and Power, 115 (July 1993) 628-633.

26. Fogler, H. S.; Elements of Chemical Reaction Engineering, Second Edition; Prentice Hall, Englewood Cliffs, NJ (1992).

27. Graham, T.; Phil. Trans. Roy. Soc. 156 (1866) 399

28. Grashoff,G.J.; Pilkington, C.E.; Corti, C.W.; "The Purification of Hydrogen – A Review of the Technology Emphasizing the Current Status of Palladium Membrane Diffusion," Platinum Metal Reviews 27 No. 4 (1983) 157-169

29. Geankoplis, C.J.; “Transport Processes and Unit Operations” Prentice Hall P T R, 1993.

30. Graven, W. M.; Long, F. J.; Kinetics and Mechanisms of the Two Opposing Reactions of the Equilibrium CO + $H_2O$ = $CO_2$ + $H_2$; J. Amer. Chem. Soc. 76 (1954) 2602.

31. Helling, R.K.; Tester, J.W.; Oxidation Kinetics of Carbon Monoxide in Supercritical Water; Energy and Fuels, 1 (1987) 417-423.

32. Holgate, H.R.; Webley, P.A.; Tester, J.W.; CO in Supercritical Water: The Effects of Heat Transfer and the Water-Gas Shift Reaction on Observed Kinetics; Energy & Fuels, 6 (1992) 586-597.

33. Holleck, G.L.; “Diffusion and Solubility of Hydrogen in Palladium and Palladium-Silver Alloys,” Journal of Physical Chemistry 74 No. 3 (Feb. 5, 1970) 503-511

34. Hsieh, H.P.; “Inorganic Membranes for Separation and Reaction”, Elsevier Science1996.

35. Hurlbert, R.C.; Konecny, J.O.; “Diffusion of Hydrogen through Palladium,” The Journal of Chemical Physics 34, No. 2 (Feb. 1961) 655-658

36. Itoh, N.; Govind, R.; Development of a Novel Oxidative Palladium Membrane Reactor; AIChE Symposium Series 268, Govind and Itoh, eds.; New York, NY 1989.

37. Itoh, N.; Xu, W.; Haraya, K.; “Basic Experimental Study on Palladium Membrane Reactors,” J. of Membrane Science 66 (1992) 149-155.

38. Itoh, N.; Xu, W.; Sathe, A.; Capability of Permeate Hydrogen through Palladium-Based Membranes for Acetylene Hydrogenation; Ind. Eng. Chem. Res. 32 (1993) 2614-2619.

39. Jemaa, N.; Shu, J.; Kaliaguine, S.; Grandjean,B.; “Thin Palladium Film Formation on Shot Peening Modified Porous Stainless Steel Substrates,” Ind. Eng. Chem. Res. 35 (1996) 973-977.

40. Katsuta, H.; Farraro, R.J.; McLellan, R.B.; “The Diffusion of Hydrogen in Palladium,” Acta Metallurgica. 27 (1979) 1111-1114

41. Keiski, R.; Salmi, T.; Niemisto, P.; Ainassaari, J.; Pohjola, V.J.; Stationary and Transient Kinetics of the High Temperature Water-Gas Shift Reaction; Applied Catalysis A: General, 137 (1996) 349-370.

42. Keiski, R.I.; Desponds, O.; Chang, Y.; Somorjai, G.A.; Kinetics of the Water-Gas Shift Reaction Over Several Alkane Activation and Water-Gas Shift Catalysts; Applied Catalysis A: General, 101 (1993) 317-338.

43. Knapton, A.; “Palladium Alloys for Hydrogen Diffusion Membranes – A Review of High Permeability Materials,” Plat. Met. Rev. 21 (1977) 44-50.

44. Koffler, S.A.; Hudson, J.B.; Ansell, G.S.; "Hydrogen Permeation Through Alpha-Palladium," Transactions of the Metallurgical Society of AIME 245 (1969) 1735-1740

45. Kusakabe, K.; Yokoyama, S.; Morooka, S.; Hayashi, J.; Nagata, H.; "Development of Supported Thin Palladium Membrane and Application to Enhancement of Propane Aromatization on Ga-Silicate Catalyst," Chemical Engineering Science 51 (1996) 3027-3032.

46. Li, Anwu; L., W.; Hughes, R.; "Charaterization and Permeation of Palladium/Stainless Steel Composite Membranes", J. Mem. Sci. 149 (1998) 259-268.

47. Liu, Y.; Dixon, A.; Ma, Y.; Moser, W.; Permeation of Ethylbenzene and Hydrogen Through Untreated and Catalytically Treated Alumina Membranes; Separation Science and Technology 25 (1990) 1511-1521.

48. Mardilovich, P.P.; She, Y.; Ma, Y.H.; Rei, M.-H.; "Defect-Free Palladium Membranes on Porous Stainless-Steel Support," AIChE Journal, 44 No. 2 (Feb. 1998) 310-322.

49. Moss, T.S.; Peachey, N.M.; Snow, R.C.; Dye, R.C.; "Multilayer Membranes for Hydrogen Separation" Int. J. Energy, Vol 23, No. 2, (1998) 99-106.

50. Netherlands Energy Research Foundation ; Combined Cycle Project – IGCC with $CO_2$ Removal Project Area – An Attractive Option for $CO_2$ Control in IGCC Systems: Water Gas Shift with Integrated Hydrogen/Carbon Dioxide Separation (WIHYS) Process – Phase 1 Proof of Principle; Alderliesten, P. T. and Bracht, M., eds.; Contract JOU2-CT92-0158, Final Report (1995).

51. Parsons Infrastructure and Technology Group; Decarbonized Fuel Plants Utilizing Inorganic Membranes for Hydrogen Separation; presented at the 12th Annual Conference of Fossil Energy Materials, May 12-14, 1998, Knoxville, Tennessee.

52. Parsons Infrastructure and Technology Group; Decarbonized Fuel Plants for Vision 21 Applications, WYODAK Coal Substitution; DOE/FETC Report, April 13, 1999.

53. Peachey, N. M.; Snow, R. C.; Dye, R. C.; Composite Pd/Ta Metal Membranes for Hydrogen Separation; Journal of Membrane Sciences (in press).

54. Perry's Chemical Engineer's Handbook, Fifth Edition, McGraw-Hill (1984).

55. Pick, M. A.; Greene, M. G.; "Uptake Rates for Hydrogen by Niobium and Tantalum: Effect of Thin Metallic Overlayers", J. of Less-Common Metals, 73 (1980) 89-95.

56. Rice, S.F., Steeper, R. R.; Aiken, J. D.; Water Density Effects on Homogeneous Water-Gas Shift Reaction Kinetics; J. Phys. Chem. A, 102(16) (1998), 2673-2678.

57. Rostrup-Nielsen, J.R.; Catalytic Steam Reforming; Chapter 1 of Catalysis Science and Technology, Vol. 5; Anderson, J. and Boudart, M., eds; Springer-Verlag (1984), 1-118.

58. Rothenberger, K.S.; Cugini, A.V.; Siriwardane, R.V.; Martello, D.V.; Poston, J.A.; Fisher, E.P.; Graham, W.J.; Balachandran, U.; Dorris, S.E.; "Performance Testing of Hydrogen Transport Membranes at Elevated Temperatures and Pressures", Am. Chem. Soc., Fuel Chem. Div., Prepr. Pap., 44(4), (1999). 914-918.

59. Shu, J.; Grandjean, B.; Kaliaguine, S.; "Methane Steam Reforming in Asymmetric Pd- and Pd-Ag/Porous SS Membrane Reactors," Applied Catalysis A: General 119 (1994) 305-325.

60. Shu, J.; Grandjean, B.; Van Neste, A.; Kaliaguine, S.; "Catalytic Palladium-based Membrane Reactors: A Review," Can. J. of Chem. Eng. 69 (1991) 1036-1060.

61. Shu, J.; Grandjean, B.; Van Neste, A.; Kaliaguine, S.; Giroir-Fendler, A.;Dalmon, J.; "Hysteresis in Hydrogen Permeation through Palladium Membranes,"J. Chem. Soc., Faraday Trans. (1996) 2475-2751.

62. Singh, C.P.; Saraf, D.N.; Simulation of High-Temperature Water-Gas Shift Reactors; Ind. Eng. Chem. Process Des. Dev. 16(3) (1977).

63. Souleimanova, R.S.; Mukastan, A.S.; Varma, A.; "Dense Pd-Composite Membranes Prepared by Electroless Plating and Osmosis: Synthesis, Characterization and Hydrogen Permeation Studies," AIChEJ (in press)

64. Steward, S.A.; "Review of Hydrogen Isotope Permeability Through Metals, Lawrence Livermore National Laboratory Report UCRL-53441, August 15, 1983.

65. Sun, Y.; Khang, S.; "Catalytic Membrane for Simultaneous Chemical Reaction and Separation Applied to a Dehydrogenation Reaction," Ind. Eng. Chem. Res. 27 (1988) 1136-1142.

66. Toda, G.; "Rate of Permeation and Diffusion Coefficient of Hydrogen Through Palladium," Journal of the Research Institute for Catalysis, Hokkaido University, 6 (1958) 13-19

67. Tsotsis, A.; Champagnie, A.; Vasileiadis, S.; Ziaka, Z.; Minet, R.; Packed Bed Catalytic Reactors; Chemical Engineering Science 47(9) (1992) 2903-2908.

68. Uemiya, S.; Sato, N.; Ando, H.; Kikuchi, E.; "The Water-Gas Shift Reaction Assisted by a Palladium Membrane Reactor", Ind. Eng. Chem. Res. 67 (1991a) 585-589

69. Uemiya, S.; Sato, N.; Ando, H.; Matsuda, T.; Kikuchi, E.; "Separation of Hydrogen through Palladium Thin Films Supported on a Porous Glass Tube," J. of Membrane Science 56 (1991c) 303-313

70. Uemiya, S.; Sato, N.; Ando, H.; Matsuda, T.; Kikuchi, E.; "Steam Reforming of Methane in a Hydrogen-Permeable Membrane Reactor," Applied Catalysis 667 (1991b) 223-230

71. Velicks, E.; Edwards, R.K.; J. Phys.Chem. 73, 683 (1969).

72. Watkins, J.; Fisher, S.; Fernandes, N.; Tsapatsis, M.; Vlachos, D.; "Fabrication of Supported Thin Film Metal Membranes for Hydrogen Separation by Reactive Deposition from Supercritical Fluids," presented at: Session T1019 - Recent Developments in New Membrane Materials II, AIChE National Meeting, Dallas, TX, Oct. 31 – Nov. 5, 1999

73. Yan S.; Maeda, H.; Kusakabe, K.; Morooka, S.; "Thin Palladium Membrane Formed in Support Pores by Metal-Organic Chemical Vapor Deposition Method and Application to Hydrogen Separation," Ind. Eng. Chem. Res. 33 (1994) 616-622